

# 1 From *cereus* to anthrax and back again: The role of the PlcR 2 regulator in the “cross-over” strain *Bacillus cereus* G9241

3

4 Shathviga Manoharan<sup>1</sup>, Grace Taylor-Joyce<sup>1</sup>, Thomas A. Brooker<sup>1</sup>, Carmen Sara Hernandez-  
5 Rodriguez<sup>2</sup>, Alexia Hapeshi<sup>1</sup>, Victoria Baldwin<sup>3</sup>, Les Baillie<sup>4</sup>, Petra C. F. Oyston<sup>3</sup> and Nicholas  
6 R. Waterfield<sup>1</sup>✦.

7

8 <sup>1</sup>Division of Biomedical Sciences, Warwick Medical School, University of Warwick, Gibbet Hill Road, Coventry, CV4  
9 7AL, United Kingdom

10 <sup>2</sup>Dpto. Microbiología y Ecología, Instituto BIOTECMED, Universitat de València, 46100 Burjassot, Spain.

11 <sup>3</sup>CBR Division, Dstl Porton Down, Salisbury, SP4 0JQ, United Kingdom

12 <sup>4</sup>School of Pharmacy and Pharmaceutical Sciences, Cardiff University, CF10 3AT, Cardiff, United Kingdom

13

14 ✦ **corresponding author (n.r.waterfield@warwick.ac.uk)**

15

16

## 17 **ABSTRACT**

18 The *plcR* gene, which encodes the pleiotropic transcriptional regulator of secreted proteins found in  
19 most members of the *Bacillus cereus* group, is truncated in all *Bacillus anthracis* isolates. The current  
20 dogma suggests this truncation was evolved to accommodate the acquisition of the anthrax toxin  
21 regulator, AtxA. However, the *B. cereus*-*B. anthracis* “cross-over” strain *Bacillus cereus* G9241, isolated  
22 from a Louisiana welder suffering from an anthrax-like infection, appears to contradict the proposed  
23 dogma as it encodes intact copies of both regulators. Here we report that when cultured at 25 °C, cell  
24 free *B. cereus* G9241 culture supernatants are cytotoxic and haemolytic to various eukaryotic cells in  
25 addition to insect haemocytes from *Manduca sexta*. However, this cytotoxic and haemolytic activity of  
26 the culture supernatant is lost when the bacteria are grown at 37 °C, behaving much like the  
27 supernatants generated by *B. anthracis*. Using a combination of genetic and proteomic approaches, we  
28 identified several PlcR-regulated toxins secreted at 25 °C. We demonstrate that a limiting step for the  
29 production of these virulence factors at 37 °C exists within the PlcR-PapR regulation circuit in strain  
30 G9241, giving rise to the temperature-dependent haemolytic and cytotoxic activity of the culture  
31 supernatants. Differential expression of the protease responsible in processing the PlcR quorum  
32 sensing activator PapR appears to be responsible for this phenotype. This study confirms that *B. cereus*  
33 G9241 is able to ‘switch’ between *B. cereus* and *B. anthracis*-like phenotypes in a temperature-  
34 dependent manner, potentially accommodating the activities of both PlcR and AtxA.

35

36 **KEYWORDS:** *Bacillus cereus* G9241, PlcR regulon, virulence factors, secretome, haemolysis

37

## 38 INTRODUCTION

39 The *Bacillus cereus* sensu lato complex is a group of genetically similar but phenotypically diverse  
40 Gram-positive, soil-borne, rod-shaped bacteria (1,2), which includes the well-studied *Bacillus anthracis*  
41 and *Bacillus cereus*. *B. anthracis* is the etiological agent of anthrax (3) while *B. cereus* can colonise  
42 hosts as diverse as insects (4) and humans, in which many strains can cause serious foodborne illness  
43 (5). Most members of the *B. cereus* group express the chromosomally encoded transcriptional regulator  
44 PlcR (Phospholipase C regulator), which controls the expression of many secreted degradative  
45 enzymes and toxins (6). However, the *plcR* gene in all *B. anthracis* isolates contains a point mutation,  
46 which frameshifts the gene and thus renders it non-functional (7). It has been proposed that the  
47 acquisition of AtxA, the mammalian responsive transcriptional regulator involved in expressing anthrax  
48 toxins, is incompatible with the activity of PlcR, leading to a selection for PlcR mutation and inactivation  
49 (7,8). Interestingly, a *B. cereus*-*B. anthracis* “cross-over” strain designated *B. cereus* G9241  
50 (hereon referred to as *BcG9241*) encodes intact copies of both *atxA* and *plcR* genes (9), suggesting  
51 this incompatibility dogma is not as straightforward as first suggested.

52  
53 *BcG9241* was isolated from a Louisiana welder, who was hospitalised with a respiratory infection  
54 resulting in a case of potentially lethal pneumonia (9). Symptoms were similar to those of inhalational  
55 anthrax. The patient also suffered with haemoptysis. *BcG9241* possesses three extrachromosomal  
56 elements: pBCX01, pBC210 and pBFH\_1 (9,10). The plasmid pBCX01 shares 99.6% sequence  
57 homology with the plasmid pXO1 from *B. anthracis* strains. pBCX01 encodes the protective antigen  
58 (PA), lethal factor (LF), oedema factor (EF) and the AtxA1 regulator. The second plasmid pBC210  
59 (previously known as pBC218) encodes for the *B. cereus* exo-polysaccharide (BPS) capsule  
60 biosynthesis genes, *bpsXABCDEFGH* (9). A novel toxin named certhrax is also encoded on the  
61 pBC210 plasmid (11,12), which has 31% amino acid sequence similarity with the LF from *B. anthracis*.  
62 Moreover, pBC210 encodes gene products with amino acid sequences bearing homology to AtxA and  
63 PA of *B. anthracis* (9). Subsequently these genes have been named *atxA2* and *pagA2*. The third  
64 extrachromosomal element pBFH\_1 (previously known as pBClin29) is a linear phagemid (9). Although  
65 the sequence is available for pBFH\_1, it is not known if it contributes to the lifestyle of *BcG9241*. Our  
66 group demonstrated by transmission electron microscopy that the pBFH\_1 phage could be produced  
67 and released into the supernatant (13). The shape of the phage particles and the dimensions of the tail  
68 and head appeared to be consistent with the Siphoviridae family (14), suggesting the pBFH\_1 is a  
69 Siphoviridae phage. Phenotypically, *BcG9241* is haemolytic and resistant to  $\gamma$ -phage like other *B.*  
70 *cereus* strains (9). Further phenotypic and genetic analyses suggested that *BcG9241* should be  
71 considered a member of the *B. cereus* sensu stricto group as it does not encode a point mutation in the  
72 *plcR* gene indicative of a *B. anthracis* strain (8).

73  
74 PlcR controls the expression of many secreted enzymes and toxins (6,7,15), with at least 45 regulated  
75 genes found in *B. cereus* type strain ATCC 14579 (16), hereon referred to as *BcATCC14579*. These  
76 secreted proteins, which contribute significantly to virulence in mice and insects (17,18), include  
77 haemolysins, enterotoxins, proteases, collagenases and phospholipases (15). Activation of PlcR

78 requires the binding of a secreted, processed and reimported form of the signalling peptide PapR (6,19–  
79 21). The *papR* gene is located downstream of *plcR* and encodes a 48-amino acid protein. PapR<sub>48</sub> is  
80 secreted from the cell via the Sec machinery and processed to a heptapeptide by the extracellular zinc  
81 metalloprotease, NprB and potentially other extracellular proteases (22). The *nprB* gene is often tightly  
82 linked to the *plcR-papR* operon, but in the opposite orientation (6,21,22). The processed form PapR<sub>7</sub> is  
83 reimported into the bacterium by the oligopeptide permease (Opp) system (23). The processed form of  
84 PapR can then bind and activate PlcR. The active PlcR-PapR complex binds to the palindromic operator  
85 sequence (PlcR box: TATGNAN4TNCATA) found in the promoter regions of the regulon genes,  
86 subsequently activating transcription of these genes (24–26). PlcR also positively auto-regulates its  
87 own transcription, which can be repressed by the sporulation factor Spo0A, facilitated by two Spo0A  
88 boxes flanking the PlcR box (27). Four distinct classes of PlcR-PapR systems have evolved and differ  
89 by the 5 C-terminal amino acids of PapR, which bind to PlcR, with PapR from one group unable to  
90 activate the transcriptional activity of PlcR from another (28).

91

92 The chromosome of *BcG9241* encodes a large range of intact exotoxin genes confirming the strain is  
93 part of the sensu stricto group (9). Several of the toxin genes are likely to be regulated by PlcR, by  
94 virtue of the presence of the PlcR-box sequence in the promoter regions (6). These include haemolysin  
95 BL (Hbl) encoded by *hblCDAB*, the tripartite non-haemolytic enterotoxin (Nhe), encoded by *nheABC*,  
96 and the enterotoxin cytotoxin K (CytK), encoded by *cytK*. These three toxins are all classed as  
97 enterotoxins and have been isolated from patients suffering from food-borne, diarrhoeal infections (29–  
98 31). Since isolating *BcG9241*, cases of anthrax-like disease caused by other non-*B. anthracis* bacteria  
99 have been reported, affecting both animals such as chimpanzees and gorillas in the Ivory Coast and  
100 Cameroon during the early 2000s (32–36), in addition to humans (9,10,37–44). Some of these isolates  
101 carry functional copies of *plcR* and *atxA* (recently reviewed in (45)); this warrants further investigation  
102 into the role of PlcR in these strains, as the loss of PlcR activity has been proposed to be crucial in  
103 anthrax disease caused by *B. anthracis*. So far, only one study on *BcG9241* has been carried out to  
104 identify how PlcR, AtxA and their respective regulons are expressed. A microarray assay carried out by  
105 (46) demonstrated that in *BcG9241* the *plcR* gene was ~2.4 fold more highly expressed in an aerobic  
106 environment compared to when exposed to CO<sub>2</sub>/bicarbonate, while in contrast, the *atxA1* gene showed  
107 higher expression in CO<sub>2</sub> by ~5.6 fold. Understanding how the PlcR-PapR regulatory circuit acts in *B.*  
108 *cereus*-*B. anthracis* “cross-over” strains may provide an insight into their evolution and give a more  
109 complete picture of the phylogeny.

110

111 Here, we describe the temperature-dependent haemolytic and cytolytic activity of *BcG9241*, caused by  
112 PlcR-controlled toxins and proteases. We also identify the limiting step in the PlcR-PapR circuit involved  
113 in preventing the expression of PlcR-regulated toxins at 37 °C. NprB is not involved in processing PapR  
114 in *BcG9241* and other *B. cereus* strains carrying functional copies of both *plcR* and *atxA*. We  
115 hypothesise that a change in the PlcR-PapR regulatory network in *BcG9241* may have allowed the  
116 carriage of intact copies of both *plcR* and *atxA*, by virtue of a temperature-dependent suppression of  
117 the PlcR-PapR circuit and the loss of the *nprB* gene.

118

## 119 RESULTS

120

### 121 ***BcG9241* culture supernatants demonstrate temperature-dependent toxicity**

122 **against a range of eukaryotic cells.** It has been previously shown in other members of the *B.*

123 *cereus* group that PlcR regulates the secretion of multiple virulence proteins, such as cytolytic toxins

124 and enzymes involved in macromolecule degradation (16,47,48). We therefore tested the haemolytic

125 activity of cell free culture supernatants from *BcG9241* cultures grown at 25 °C and 37 °C to sheep

126 erythrocytes. We tested the effect of growth at 25 °C and 37 °C to partially emulate environmental and

127 mammalian host conditions, respectively. Filtered supernatants were extracted from cultures grown to

128 exponential phase (OD<sub>600</sub>=0.5) and stationary phase (OD<sub>600</sub>=1.5). From 25 °C cultures, the

129 supernatants from exponential and stationary phases demonstrated haemolytic activity to red blood

130 cells (RBCs), above the 75% level by comparison to the expected lysis from the positive control (1%

131 Triton X100) (**Fig 1**). In contrast, supernatants from *BcG9241* grown at 37 °C showed very little lytic

132 activity (**Fig 1**). This led us to the hypothesis that *BcG9241* ‘switches’ its phenotype from a haemolytic

133 *B. cereus*-like phenotype at 25 °C to a non-haemolytic *B. anthracis*-like phenotype at 37 °C.

134

135 We expanded the study to test the toxicity of cell free culture supernatants from a range of *Bacillus*

136 cultures grown at 25 °C against *ex vivo* *Manduca sexta* haemocytes. Filtered supernatants were

137 extracted from cultures grown for 16 h. Microscopic examination showed that supernatants from the

138 reference strain *BcATCC14579*, *BcG9241* and *BcG9241* ΔpBCX01 (in which the plasmid had been

139 cured) caused extensive lysis of the *M. sexta* haemocytes (**Fig S1A**). In contrast, supernatants from

140 *Bacillus thuringiensis* 407 Cry<sup>-</sup> Δ*plcR* (*Bt* Δ*plcR*) mutant strain were innocuous, showing no difference

141 from the negative buffer control (**Fig S1A**). *Bt* Δ*plcR* is an accepted Δ*plcR* *B. cereus* model as the

142 crystal toxin plasmid has been cured (27). The cytotoxicity observed with *BcG9241* and *BcG9241*

143 ΔpBCX01 indicated that cytotoxins were secreted by both strains and is possibly unaffected by the

144 presence of pBCX01 plasmid at 25 °C (**Fig S1A**).

145

146 We quantified the effect of supernatants from these same strains using haemocyte cell viability assays.

147 We also expanded the study to include supernatants from the *B. anthracis* Sterne strain, which lacks

148 the pXO2 plasmid (hereon referred to as *Ba* St). Like all *B. anthracis* strains, *Ba* St has a frame-shifted

149 copy of the *plcR* gene. From 25 °C grown cultures, we observed cytotoxicity responses consistent with

150 the microscopic examinations (**Fig S1B**), with the supernatants of *BcATCC14579*, *BcG9241* and

151 *BcG9241* ΔpBCX01, all showing potent toxicity. In contrast, supernatants from *Ba* St and *Bt* Δ*plcR*

152 showed little or no cytotoxicity (**Fig S1B**). However, when grown at 37 °C, cytotoxicity of *BcG9241* and

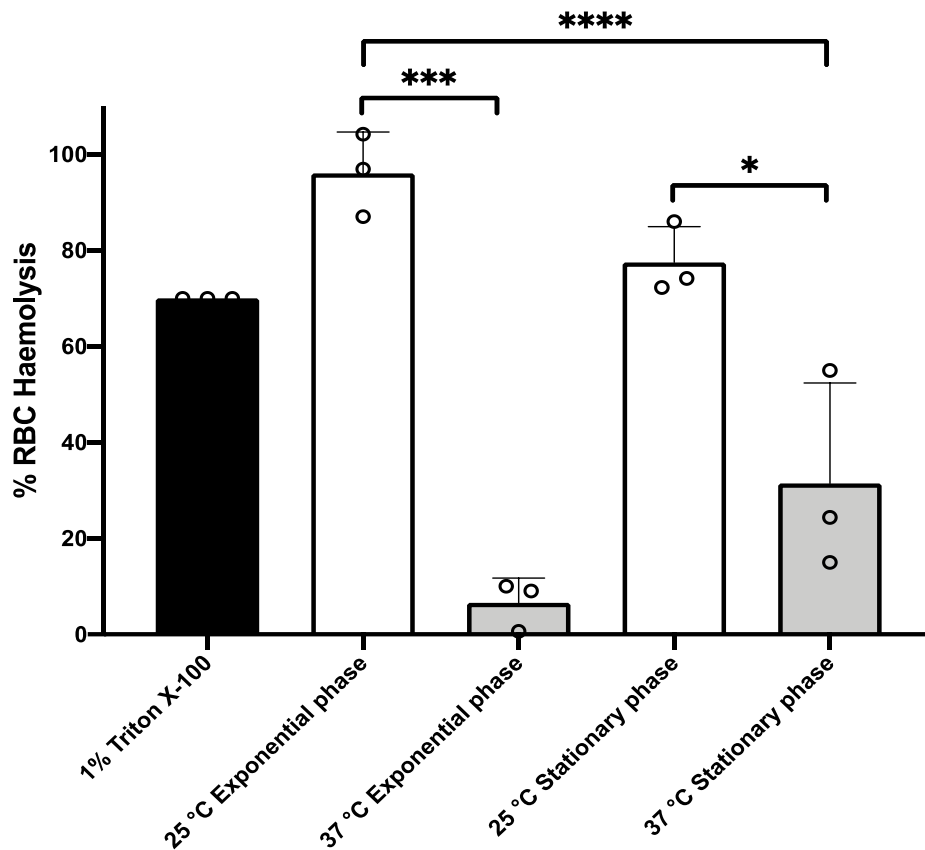
153 *BcG9241* ΔpBCX01 supernatants was highly attenuated, to levels no different from those of the *Ba* St

154 and *Bt* Δ*plcR* supernatants (**Fig S1C**). Cytotoxicity of the *BcATCC14579* supernatant was still observed

155 at 37 °C (**Fig S1C**). Temperature-dependent cytotoxic activity of *BcG9241* and *BcG9241* ΔpBCX01

156 supernatants were also observed in a range of mammalian cells including T2-lymphocytes,

157 polymorphonuclear leukocytes and macrophages (using supernatant extracted from *Bacillus* cultures  
158 grown for 16 h), which re-capitulated the trend seen with the insect haemocytes (**Fig S2**).



159 **Figure 1: *BcG9241* supernatant is significantly more toxic to sheep RBCs, when extracted from**  
160 **a 25 °C grown culture compared to a 37 °C grown culture.** The haemolysis assay was conducted  
161 by incubating *BcG9241* supernatant with 4% RBCs for 1 hour at 37 °C. The OD<sub>540</sub> was measured, and  
162 RBC lysis was calculated as a % of expected RBC lysis by Triton X-100 (1% v/v). Stars above columns  
163 represent significance levels. \* denotes an unpaired t test with a p-value of 0.0232; \*\*\* denotes a  
164 Welch's t test with a p-value of 0.0003; \*\*\*\* denotes an ordinary one-way ANOVA with a p-value of  
165 <0.0001. Error bars denote one standard deviation, and all samples were to an n=3.

166

167

### 168 **Temperature and growth phase-dependent proteomic analysis of *BcG9241***

169 **culture supernatants.** In order to investigate the potential cytolytic and haemolytic factors  
170 secreted by *BcG9241*, we analysed the proteomic profiles of supernatants from cultures grown at 25  
171 °C and 37 °C in LB broth, taken from both mid-exponential (OD<sub>600</sub> = 0.5) and stationary growth phases.  
172 For stationary phase, *BcG9241* cultures supernatant were extracted after 10 hours growth at 25 °C and  
173 after 7 hours growth at 37°C (13). Proteins were run through nanoLC-ESI-MS and peptide reads were  
174 counted using MaxQuant (Max Planck Institute). Comparisons were made using the Perseus software

175 (Max Planck Institute) and plotted as the difference in proteins expressed between the two  
176 temperatures. The full datasets generated can be seen in the **Supplementary Dataset S1 and S2**.

177

178 A principal component analysis (PCA) was generated to show the variance between all biological  
179 replicates of the *BcG9241* supernatants collected from both exponential- and stationary phases. The  
180 PCA plots revealed that protein extracts from the exponential phase supernatants overlap with each  
181 other, not forming distinct clusters and are highly reproducible (**Fig S3**). The plot also showed that  
182 growth temperature affected the protein profiles more significantly at stationary phase compared to  
183 exponential phase (**Fig S3**). Furthermore, protein profiles extracted from stationary phase growth at 37  
184 °C were more variable than those from other conditions (**Fig S3**).

185

186 **A diverse and abundant toxin “profile” was secreted at 25 °C, while high levels of phage proteins**  
187 **were secreted at 37 °C during exponential growth phase of *BcG9241*.** With the cut-off criteria of p-  
188 value < 0.05 and a minimum 2-fold change in protein level, 33 supernatant proteins were identified as  
189 being significantly more abundant at 25 °C compared to 37 °C. Of these, 11 of the 12 most highly  
190 expressed are known toxin homologs (**Table 1** and **Fig S4**). This included all components of the Hbl  
191 toxin encoded by the *hbl* operon AQ16\_4930 – 4933 (**Fig S4-purple arrows**). Other known cytotoxic  
192 proteins were also abundant in the supernatant at 25 °C compared to 37 °C, including the Nhe toxin  
193 encoded by the *nhe* operon AQ16\_658 – 660 (**Fig S4-green arrows**), a collagenase (AQ16\_1941), a  
194 thermolysin metalloproteinase (AQ16\_5317), phospholipase C (Plc, AQ16\_1823) and CytK  
195 (AQ16\_1392).

196

197 Conversely, at 37 °C, the secretome contained negligible levels of these cytotoxic proteins (if present  
198 at all). There was, however, an abundance of phage capsid proteins encoded by the pBFH\_1 phagemid  
199 at 37 °C compared to 25 °C (**Fig S4-black arrows**). More specifically 25 proteins were found to be  
200 more abundant in the secretome at 37 °C compared to 25 °C. The 10 most abundant proteins at 37 °C  
201 compared to 25 °C were encoded by the pBFH\_1 phagemid (**Table 1**). Proteins from an operon of  
202 WxL-domain cell wall-binding proteins were also seen to be more abundant at 37 °C compared to 25  
203 °C (AQ16\_3217 – 3219).

204

205 **The temperature dependent *BcG9241* secretome at stationary growth phase.** Between 25 °C and  
206 37 °C, 51 proteins showed temperature dependent differences (**Fig 2B**). Unlike the mid-exponential  
207 observations, the more abundant proteins in the 25 °C stationary phase supernatants were not all  
208 cytotoxins, although several enzymes were present (**Table 1**). In fact, of the 11 toxins seen to be more  
209 abundant at 25 °C during exponential phase growth, only AQ16\_5317 was identified at higher levels at  
210 25 °C during stationary phase. This is a thermolysin metalloproteinase, which has a PlcR-box present  
211 in the promoter region (**Table S1**), and is over 200-fold more abundant at 25 °C. The relevance of this  
212 is discussed below. Several of the more abundant proteins (e.g. AQ16\_3254, 4226, 374) identified were  
213 likely cellular proteins, possibly indicating greater autolysis at 25 °C compared to 37 °C. The top 5  
214 proteins more abundant in 37 °C compared to 25 °C supernatants were all extracellular enzymes

215 including two chitinases, a hydrolase, a glucanase and a collagenase (**Table 1**). In addition, a matrixin  
 216 family protein (AQ16\_4915), another extracellular enzyme, was also identified as 4.3 log<sub>2</sub>-fold higher  
 217 at 37 °C. Again, we saw cellular components including 50S ribosome subunit proteins and RecA, which  
 218 possibly signified cell lysis. Only one of the phage capsid proteins identified as higher at 37 °C in the  
 219 exponential phase secretome, Gp34 (AQ16\_5824), was significantly higher at 37 °C in stationary  
 220 phase.

221  
 222

223 **Table 1:** The 15 most abundant toxins at higher levels at the two temperature in the secretome of  
 224 BcG9241 during exponential growth and stationary phase. The significance cut-off criteria used was a  
 225 p-value of <0.05 and a minimum of a 2-fold change in protein level.

226

Log <sub>2</sub> -Fold Change	25 °C > 37 °C at exponential phase	Gene	Gene Loci (AQ16_)
6.46	Haemolysin BL lytic component L2		4931
5.88	Non-haemolytic enterotoxin binding component	<i>nheC</i>	658
5.67	Hemolysin BL-binding component	<i>hblA</i>	4932
4.41	Collagenase family protein		1941
4.31	Extracellular ribonuclease	<i>bsn</i>	4754
3.98	Hemolysin BL-binding component	<i>hblB</i>	4933
3.93	Non-hemolytic enterotoxin lytic component L2	<i>nheA</i>	660
3.84	Thermolysin metalloproteinase, catalytic domain protein		5317
3.77	Non-hemolytic enterotoxin lytic component L1	<i>nheB</i>	659
3.57	Haemolysin BL lytic component L1		4930
3.20	Phospholipase C	<i>olc</i>	1823
2.69	Cytotoxin K	<i>cytK</i>	1392
2.49	THUMP domain protein		931
2.44	Probable butyrate kinase	<i>buk</i>	3880
2.42	DEAD-box ATP-dependent RNA helicase	<i>cshA</i>	2258
<b>37 °C &gt; 25 °C at exponential phase</b>			
5.27	Phage family protein	<i>gp49</i>	5822
4.96	Putative phage major capsid protein	<i>gp34</i>	5824
4.53	Prophage minor structural protein		5836
4.32	Putative gp14-like protein	<i>gp14</i>	5832
4.31	N-acetylmuramoyl-L-alanine amidase family protein		5839
3.65	Phage tail family protein		5835
3.40	Putative major capsid protein	<i>gpP</i>	5831
2.89	Uncharacterized protein		5823
2.36	WxL domain surface cell wall-binding family protein		3215
2.34	WxL domain surface cell wall-binding family protein		3217
2.33	Phage antirepressor KilAC domain protein		5855
2.30	Dihydropteroate synthase	<i>folP</i>	2448
2.19	Zinc-binding dehydrogenase family protein		318
2.07	WxL domain surface cell wall-binding family protein		3218
1.95	Toxic anion resistance family protein		2068
<b>25 °C &gt; 37 °C at stationary phase</b>			
7.83	Thermolysin metalloproteinase, catalytic domain protein		5317
4.86	Transglutaminase-like superfamily protein		1487
4.54	UDP-N-acetylglucosamine 1-carboxyvinyltransferase	<i>murA</i>	2685

4.51	Ribonuclease J	<i>rnjA</i>	2375
4.51	Ornithine aminotransferase	<i>rocD</i>	1349
4.16	Pyruvate carboxylase	<i>pyc</i>	4104
4.10	Malic enzyme, NAD binding domain protein		3400
4.01	CTP synthase	<i>pyrG</i>	2681
3.95	Glycerophosphoryl diester phosphodiesterase family protein		4572
3.73	Leucine--tRNA ligase	<i>leuS</i>	3254
3.66	Viral enhancin family protein		2918
3.66	Subtilase family protein		4301
3.16	50S ribosomal protein L2	<i>rplB</i>	2391
3.16	Aldo/keto reductase family protein		2308
3.14	Sphingomyelin phosphodiesterase	<i>sph</i>	1822
<b>37 °C &gt; 25 °C at stationary phase</b>			
9.19	Chitinase A1	<i>chiA1</i>	2089
7.85	Putative hydrolase		2662
7.31	Glucanase		5335
6.99	Collagenase family protein		4546
5.67	Chitinase A		4342
4.83	Peptide ABC transporter		2309
4.54	Calcineurin-like phosphoesterase family protein		4913
4.43	Urocanate hydratase	<i>hutU</i>	4415
4.31	Single-stranded DNA-binding protein	<i>ssb</i>	2546
4.28	Matrixin family protein		4915
3.77	3-hydroxyacyl-[acyl-carrier-protein] dehydratase FabZ	<i>fabZ</i>	2750
3.56	Formate acetyltransferase	<i>ptfB</i>	2025
3.52	Ribose-phosphate pyrophosphokinase	<i>prs</i>	2472
3.26	Putative phage major capsid protein		5824
3.22	50S ribosomal protein L4	<i>rplD</i>	2393

227

## 228 Temperature-dependent cell proteome analysis of exponentially growing

229 **BcG9241 cells.** The greatest temperature-dependent change in secreted toxin profiles was seen in  
 230 exponentially growing cells. Therefore, to investigate the potential role of PlcR in the temperature-  
 231 dependent regulation of toxin secretion, and any relationship between protein synthesis and secretion,  
 232 a proteomic analysis of whole cells was performed. The same samples used for the supernatant  
 233 proteomic analysis were used for this, allowing for direct correlation of the datasets. The full datasets  
 234 generated can be seen in the **Supplementary Dataset S3**.

235

## 236 No build-up of toxins was observed in the cellular proteome of BcG9241 at 37 °C exponential

237 **phase.** With a cut-off criteria of p-value < 0.05 and a minimum 2-fold change in protein level, 67 proteins  
 238 were found to be significantly more abundant at 25 °C compared to 37 °C. The most abundant proteins  
 239 at 25 °C compared to 37 °C included cold shock proteins CspA and YdoJ family proteins (**Table 2** and  
 240 **Fig S5**). Only two of the toxin proteins seen at higher levels at 25 °C in comparison to 37 °C in the  
 241 secretome were also significantly higher in the cell proteome, NheA and NheB (AQ16\_659 and 660).

242

243 51 proteins were found to be significantly more abundant at 37 °C compared to 25 °C (**Table 2**). Proteins  
 244 from an operon of WxL-domain cell wall-binding proteins were seen to be more abundant at 37 °C



245 (AQ16\_3217 – 3219). In addition, various heat stress response proteins were also identified as higher  
246 at 37 °C. These include: AQ16\_3857, a DNA repair protein; AQ16\_512, a DNA protection protein and  
247 a thermosensor operon, AQ16\_3712 – 3714, involved in protein refolding. Interestingly, despite the  
248 significantly increased abundance in the secretome, only two proteins encoded on the pBFH\_1  
249 phagemid (AQ16\_5849 and \_5858) showed increased abundance in the cell proteome, both of which  
250 are uncharacterised.

251

252 A build-up of toxins from the cell proteome at 37 °C was not observed, demonstrating that temperature-  
253 dependent toxin expression is not regulated at the level of secretion. PlcR was detected at both  
254 temperatures with no significant difference in abundance levels.

255 **Table 2:** Top 15 cellular proteins that are more abundant at each temperature in exponentially growing  
 256 *BcG9241*. The significance cut-off criteria used was a p-value of <0.05 and a minimum 2-fold change  
 257 in protein level.

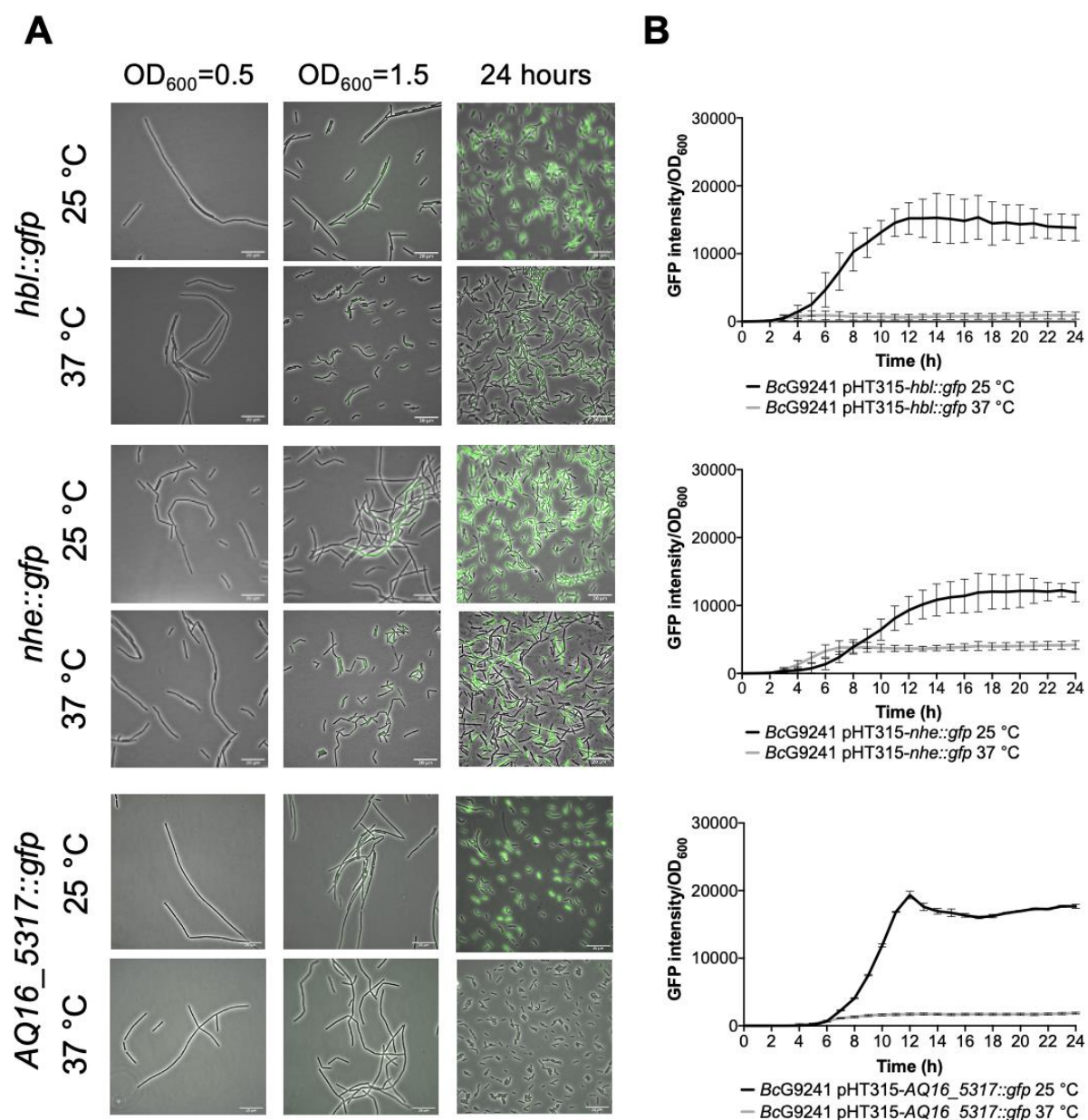
Log <sub>2</sub> -Fold Change	25 °C > 37 °C at exponential phase	Gene	Gene Loci (AQ16_)
5.09	Major cold shock protein	<i>cspA</i>	1368
4.72	Uncharacterized protein		4251
4.48	Cold-inducible YdjO family protein		175
4.10	Uncharacterized protein		4821
3.18	Transglutaminase-like superfamily protein		1487
3.06	Flagellar motor switch FliM family protein		858
2.77	FMN-dependent NADH-azoreductase	<i>azoR4</i>	2611
2.57	Uncharacterized protein		1372
2.47	Hemolytic enterotoxin family protein		659
2.41	Uncharacterized protein		1559
2.21	Major cold shock protein	<i>cspA</i>	174
2.20	SET domain protein		2908
2.19	Transposase family protein		1725 / 4355
2.15	Rhodanese-like domain protein		1704
2.09	Hemolytic enterotoxin family protein	<i>nheA</i>	660
<b>37 °C &gt; 25 °C at exponential phase</b>			
4.34	WxL domain surface cell wall-binding family protein		3218
3.74	Uncharacterized protein		3219
2.87	Formate acetyltransferase	<i>pflB</i>	2025
2.73	Uncharacterized protein		1429
2.29	DNA repair protein	<i>recN</i>	3857
2.27	DNA protection during starvation protein 1	<i>dps1</i>	512
2.25	Uncharacterized protein		5765
2.25	Pyruvate formate-lyase-activating enzyme	<i>pflA</i>	2024
2.23	L-lactate dehydrogenase	<i>ldh</i>	3111
2.166	CamS sex pheromone cAM373 family protein		2171
2.09	L-asparaginase, type I family protein		4939
1.98	Heat-inducible transcription repressor	<i>hrcA</i>	3712
1.97	Uncharacterized protein		5849
1.96	Membrane MotB of proton-channel complex MotA/MotB family protein		3490
1.84	Periplasmic binding family protein		1888

258  
 259 **Analysis of PlcR-controlled toxin expression in *BcG9241*.** Haemolytic and cytolytic  
 260 assays have suggested that *BcG9241* containing a functional copy of the *plcR* gene show temperature-  
 261 dependent toxicity. Hbl, Nhe, Plc, CytK and a thermolysin metalloproteinase (AQ16\_5317), which are  
 262 regulated by the PlcR-PapR circuit (16), were detected with high abundance in the secretome analysis  
 263 at 25 °C compared to 37 °C. In order to confirm the temperature-dependent toxin and protease

264 production, a panel of transcription-translation reporter plasmids were made, in which the promoter  
265 regions and the first 24 bp of the coding sequence of *hbl*, *nhe*, *plc*, *cytK* and *AQ16\_5317* were  
266 genetically fused in frame to a *gfp* gene with no start codon (referred to hereon as *hbl::gfp*, *nhe::gfp*,  
267 *plc::gfp*, *cytK::gfp* and *AQ16\_5317::gfp*). Note that only eight N-terminal amino acids from the ORF  
268 were cloned as it is not sufficient to serve as a Sec-dependant secretion signal for the toxins, preventing  
269 the GFP from being secreted. For comparison, GFP reporters of PlcR-regulated toxins were also  
270 constructed for *BcATCC14579* from homologous regions. Each of the reporter constructs were then  
271 transformed into the relevant *B. cereus* strain and examined using fluorescence microscopy and  
272 microtitre plate reader assays to assess the expression patterns across growth phases at 25 °C and 37  
273 °C, when grown in LB while maintaining plasmid marker selection. The rate of change in fluorescence  
274 ( $\Delta\text{GFP}/\text{OD}_{600}$ ) was calculated every hour by subtracting the fluorescence at a given time point by the  
275 fluorescence of the previous time point. This would reveal when the biggest change in GFP expression  
276 occurs across the growth phase.

277  
278 From the microscopy images, the expression of the toxin reporters in *BcG9241* was not detected during  
279 mid-exponential phase at 25 °C and 37 °C (**Fig 2A** and **Fig S6**). However, by quantifying the GFP  
280 intensity of *B. cereus* strains containing the reporters, there were cells with higher fluorescence  
281 compared to the control cells (being above the threshold), suggesting that GFP, and therefore the PlcR-  
282 regulated proteins were being expressed. The mean GFP intensity of individual cells quantified was  
283 higher at 25 °C compared to 37 °C for *hbl::gfp*, *nhe::gfp* and *cytK::gfp* (**Fig S8**). Once reaching stationary  
284 phase, the difference in the expression of the toxin reporters in *BcG9241* was more pronounced  
285 between 25 °C and 37 °C (**Fig 2A** and **Fig S6**). From GFP intensity quantification of individual cells  
286 from the micrographs, the mean GFP intensity of *hbl::gfp*, *nhe::gfp*, *plc::gfp* and *AQ16\_5317::gfp* at the  
287 onset of stationary phase and 24 hours was higher at 25 °C compared to 37 °C in *BcG9241* (**Fig S7**).  
288 It is interesting to note that *BcG9241* cells formed filamentous-like structures during exponential phase  
289 which reverted to shorter vegetative rod morphologies once stationary phase was reached.

290  
291 When the GFP intensity/ $\text{OD}_{600}$  of *BcG9241* harbouring the PlcR-regulated toxin reporters was  
292 monitored with a microtitre plate reader over 24 hours (**Fig 2B** and **Fig S6**), the GFP expression was  
293 greater at 25 °C compared to 37 °C for *hbl::gfp*, *nhe::gfp*, *plc::gfp* and *AQ16\_5317::gfp* while the  
294 expression of *cytK::gfp* appeared similar between both temperatures. By calculating the rate of change  
295 in fluorescence ( $\Delta\text{GFP}$ ), a large and broad  $\Delta\text{GFP}$  peak was observed at 25 °C while the peak appeared  
296 tighter at 37 °C for *hbl::gfp*, *nhe::gfp*, *plc::gfp* and *AQ16\_5317::gfp* (**Fig S8**). In comparison, expression  
297 of *hbl::gfp*, *nhe::gfp* and *BC\_2735::gfp* (*BC\_2735* has a 97% identity to *AQ16\_5317* using BLASTP) in  
298 *BcATCC14579* appeared to be similar at 25 °C and 37 °C, while the expression of *plc::gfp* and *cytK::gfp*  
299 was temperature-dependent (**Fig S9**).



300

301 **Figure 2: Temperature dependent expression of PlcR-regulated toxins and enzymes in *BcG9241***  
 302 **using GFP reporters.** (A) A representative selection of microscopy images of the transcription-  
 303 translation GFP reporters of PlcR-regulated toxins for *BcG9241* taken at three different time points:  
 304 mid-exponential phase which is 2 hours at 37 °C and 5 hours at 25 °C (OD<sub>600</sub>=0.5), early stationary  
 305 phase which is 4 hours at 37 °C and 7 hours at 25 °C (OD<sub>600</sub>=1.5) and 24 hours. (B) **Fluorescence of**  
 306 **toxin reporters over time in LB.** GFP intensity/OD<sub>600</sub> and change in GFP ( $\Delta$ GFP/OD<sub>600</sub>) of *BcG9241*  
 307 containing PlcR-regulated toxin reporters over 24 hours growth in 100  $\mu$ l volume LB media at 25 °C (in  
 308 black) and 37 °C (in grey). Each line represents the mean of three biological replicates with three  
 309 technical replicates each and error bars denote standard deviation.

310

311 **Population level analysis of PlcR and PapR expression in BcG9241.** Subsequently,  
312 we expanded the analysis by including a panel of transcription-translation reporter plasmids for PlcR  
313 and PapR in *BcG9241* and *BcATCC14579*. The promoter regions and the first 24 bp of the coding  
314 sequence of *plcR* and *papR* were genetically fused in frame to a *gfp* gene with no start codon (referred  
315 to hereon as *plcR::gfp* and *papR::gfp*). Note that only eight N-terminal amino acids from the ORF were  
316 cloned as it is not sufficient to serve as a Sec-dependent secretion signal for PapR and to make sure  
317 that the PlcR protein was not interfering with the GFP protein. Each of the reporter constructs were then  
318 transformed into the relevant *B. cereus* strain and examined using fluorescence microscopy to assess  
319 the expression patterns across growth phases at 25 °C and 37 °C, when grown in LB and maintaining  
320 plasmid marker selection.

321  
322 **Expression of PlcR is not temperature dependent.** Expression of *plcR::gfp* was first observed during  
323 early stationary phase at 25 °C and 37 °C (**Fig 3A**). By 24 hours, levels of *plcR::gfp* increased at both  
324 temperatures, with a high level of population heterogeneity in expression within the cell population. The  
325 cells that expressed *plcR::gfp*, also did so at a high level. As observed in *BcG9241*, expression of  
326 *plcR::gfp* in *BcATCC14579* was also heterogeneous within the cell population (**Fig 3A**). Image analysis  
327 provided an objective quantification of this heterogeneous expression observed within the cell  
328 population, with a small number of cells expressing *plcR::gfp* in both *B. cereus* strains (**Fig S10**).

329  
330 There is a possibility that the population heterogeneity observed for the expression of *plcR::gfp* could  
331 be due to cell death or an error from the reporter itself. To determine whether the *plcR::gfp* expression  
332 was indeed originated from a minority of cells, some potential issues were analysed. The shuttle vector  
333 used for the reporter pHT315 encodes an erythromycin resistance gene, and therefore the antibiotic  
334 was added to maintain selection. To rule out heterogeneity due to cell death, propidium iodide staining  
335 was carried out. Cell viability is assessed when propidium iodide penetrates damaged membranes  
336 binding to nucleic acid, leading to fluorescence. At early stationary phase, only a few cells were stained  
337 by propidium iodide while within a large population of live cells, a small proportion of cells expressed  
338 *plcR::gfp* (**Fig S11**). This confirms the heterogeneous expression of *plcR::gfp* was indeed originated  
339 from a small subpopulation of live cells and this is not a consequence of cell death in any non-reporter  
340 expressing cells.

341  
342 **PapR in BcG9241 is highly expressed at 37 °C compared to 25 °C.** Expression of *papR::gfp* was  
343 first noticed during early stationary phase at 25 °C and 37 °C. Levels of *papR::gfp* expression greatly  
344 increased by 24 hours, with stronger fluorescence observed by microscopy at 37 °C compared to 25  
345 °C (**Fig 3B**). Image analysis has provided an assessment of the expression observed within the cell  
346 population, with a sub-population of cells expressing *papR::gfp* at 25 °C. In *BcG9241* and  
347 *BcATCC14579*, the mean GFP expression was higher at 37 °C compared to 25 °C (**Fig S10**).

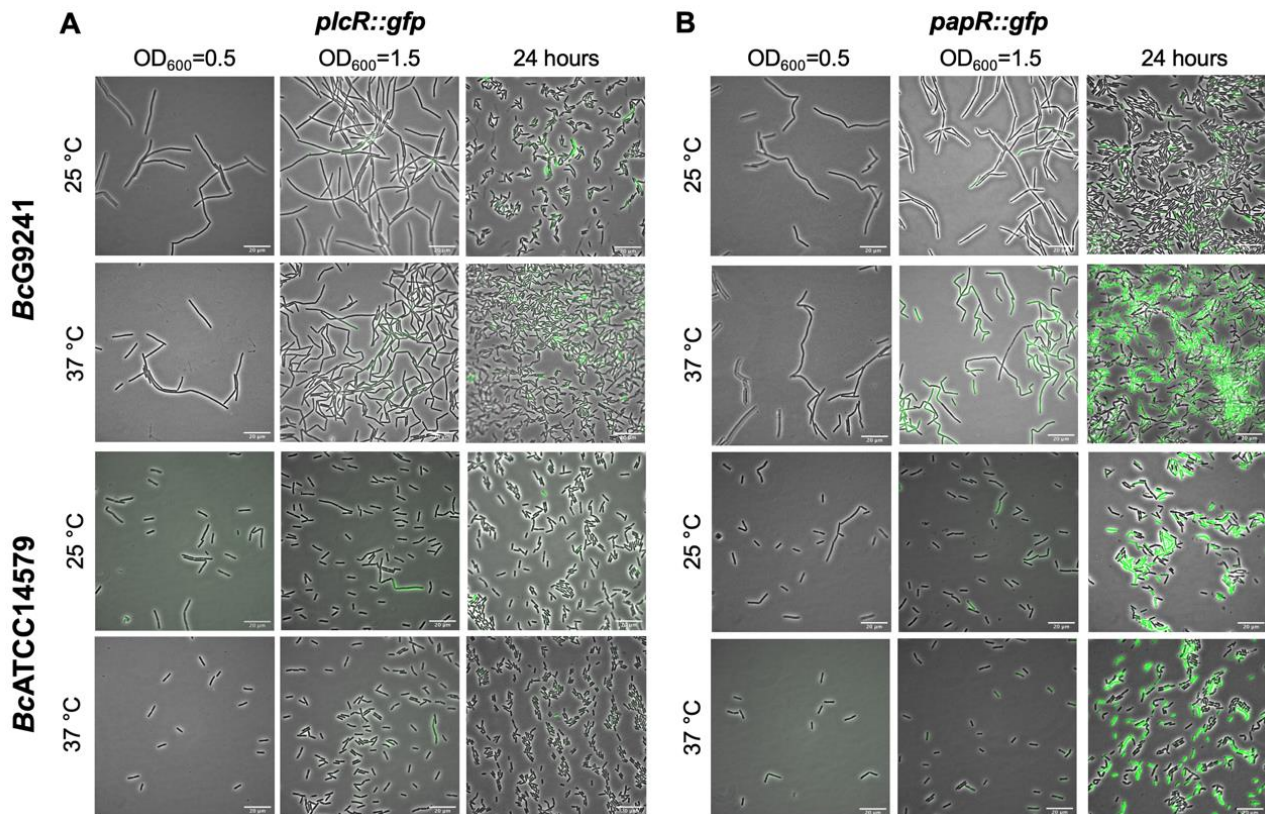


**Figure 3: A representative selection of microscopy images of *BcG9241* and *BcATCC14579* harbouring the transcription-translation GFP reporters of *plcR::gfp* and *papR::gfp*.** Micrographs were taken at three different time points: mid-exponential phase which is 2 hours at 37 °C and 5 hours at 25 °C ( $OD_{600}=0.5$ ), early stationary phase which is 4 hours at 37 °C and 7 hours at 25 °C ( $OD_{600}=1.5$ ) and 24 hours. Scale bar = 20  $\mu$ m.

348

349 **The import of mature PapR<sub>7</sub> is functional at 25 °C and 37 °C in *BcG9241*.** A build-  
350 up of toxin proteins in the cell proteome at 37 °C was not detected, suggesting that temperature-  
351 dependent toxin expression is not regulated at the level of secretion. This led us to investigate whether  
352 the import of mature PapR is not functional at 37 °C, causing the temperature-dependent haemolysis  
353 and cytolysis phenotypes observed in *BcG9241*. To understand whether the import system is functional  
354 at 37 °C, a haemolysis assay was carried out using supernatants of *B. cereus* cultures grown at 25 °C  
355 and 37 °C with mature synthetic PapR peptides added exogenously. Previous studies have  
356 demonstrated that the heptapeptide PapR<sub>7</sub> is the mature form of the quorum sensing peptide (22,28)  
357 and therefore synthetic peptides of this form (*G9241* PapR<sub>7</sub>= SDLPFEH, *ATCC14579* PapR<sub>7</sub>=  
358 KDLPFEY) were used.

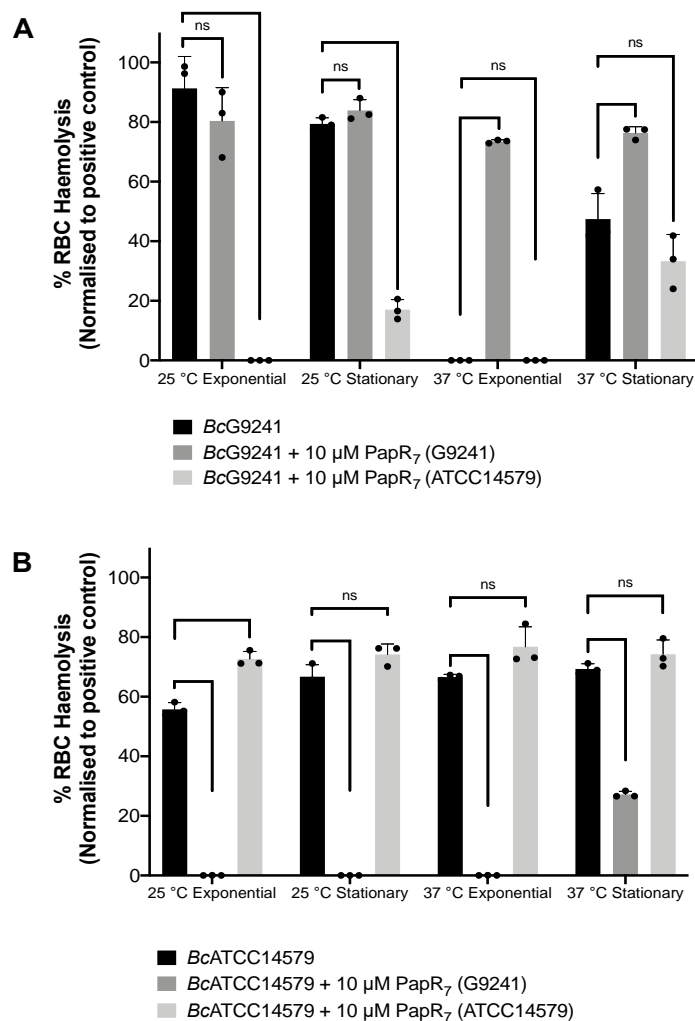
359

360 At 25 °C, with the addition of exogenous self PapR<sub>7</sub> (i.e., adding *G9241* PapR<sub>7</sub> into cultures of *BcG9241*  
361 or adding *ATCC14579* PapR<sub>7</sub> into cultures of *BcATCC14579*), no significant change in haemolytic  
362 activity of the mid-exponential supernatants of *BcG9241* was observed, compared to the absence of  
363 exogenous PapR<sub>7</sub>. Nevertheless, haemolytic activity was still observed with/without the addition of the

364 cognate PapR<sub>7</sub> from supernatants collected at 25 °C in both *BcG9241* and *BcATCC14579* (**Fig 4**). In  
365 comparison, upon the addition of exogenous PapR a significant change in haemolytic activity of the  
366 mid-exponential supernatant of *BcATCC14579* was observed, compared to the absence of exogenous  
367 PapR<sub>7</sub>. At 37 °C, with the addition of cognate PapR<sub>7</sub>, there was a significant increase in haemolytic  
368 activity with the mid-exponential and stationary phase *BcG9241* supernatant (**Fig 4**). This suggests that  
369 PapR<sub>7</sub> can get taken into the cell through an import system at 37 °C. In comparison, upon the addition  
370 of exogenous cognate PapR<sub>7</sub>, no significant change in haemolytic activity of the mid-exponential  
371 supernatant of *BcATCC14579* was observed, compared to the absence of exogenous PapR<sub>7</sub>.

372  
373 Addition of exogenous non-self PapR<sub>7</sub> molecules in *BcG9241* and *BcATCC14579* (i.e., adding G9241  
374 PapR<sub>7</sub> into cultures of *BcATCC14579* or adding ATCC14579 PapR<sub>7</sub> into cultures of *BcG9241*) led to a  
375 decrease in haemolytic activity at both temperatures (**Fig 4**). This implies that the correct PapR<sub>7</sub> is  
376 required for the expression of toxins, and that a non-self cognate variant of the peptide can actually  
377 interfere with the native PlcR-PapR circuit.

378  
379 Subsequently, we wanted to observe how the addition of the synthetic PapR<sub>7</sub> would affect the  
380 expression of PlcR-regulated toxins in *BcG9241* at 37 °C using the GFP reporters we have available.  
381 At 25 °C, addition of the cognate PapR<sub>7</sub> to *BcG9241* led to a slight increase in expression of *nhe::gfp*,  
382 no change in expression of *plc::gfp* and *cytK::gfp* and a decrease in expression of *hbl::gfp*. A decrease  
383 in the expression of *hbl::gfp* was still observed when lower concentrations of synthetic PapR were added  
384 to *BcG9241* cultures (data not shown). At 37 °C, addition of cognate PapR<sub>7</sub> to *BcG9241* led to a  
385 dramatic increase in expression of Nhe, Plc and CytK. This suggests that the processed PapR can  
386 indeed get imported into cells at 37 °C. There is no significant increase in *hbl::gfp* expression with the  
387 addition of PapR<sub>7</sub> at 37 °C (**Fig S12**) suggesting an additional level of regulation for these genes.



388 **Figure 4: The effect of exogenous PapR<sub>7</sub> in *BcG9241* and *BcATCC14579*.** 10  $\mu$ M synthetic PapR<sub>7</sub>  
 389 (G9241 PapR<sub>7</sub>= SDLPFEH, ATCC14579 PapR<sub>7</sub>= KDLPFEY) were added when the bacterial culture  
 390 was inoculated from OD<sub>600</sub>=0.005. Supernatant was extracted from mid-exponential and stationary  
 391 phase growing *B. cereus* G9241. Supernatant was filter-sterilised and incubated with 4% RBCs for 1  
 392 hour. OD<sub>540</sub> was measured and RBC lysis was calculated as a percentage of expected RBC lysis,  
 393 normalised with 70 % lysis from 1 % (w/w) Triton X-100. Error bars denote one standard deviation,  
 394 and all samples were to an n=3. \* [P < 0.05], \*\* [P < 0.01], \*\*\* [P < 0.001] and \*\*\*\* [P < 0.0001] as  
 395 determined by unpaired t-test, with Welch's correction.

396

### 397 **The PapR maturation process is potentially preventing the expression of PlcR-**

398 **controlled toxins in *BcG9241* at 37 °C.** The import of mature PapR does not appear to be a  
 399 limiting factor involved in the temperature-dependent toxin expression phenotype. Consequently, there  
 400 is a possibility that the protease(s) involved in processing PapR represents the limiting step within the  
 401 PlcR-PapR circuit in *BcG9241*. In *B. cereus*, it has been shown that the neutral protease NprB is  
 402 involved in processing the pro-peptide PapR<sub>48</sub> into the shorter and active form PapR<sub>7</sub> (22). In the *B.*  
 403 *cereus* and *B. thuringiensis* genome, the gene *nprB* is found adjacent to *plcR* and transcribed in the  
 404 opposite orientation (6,21,22). To identify whether *BcG9241* and other *B. cereus*-*B. anthracis* “cross-  
 405 over” strains have a functional copy of *nprB*, a synteny analysis using SyntTax



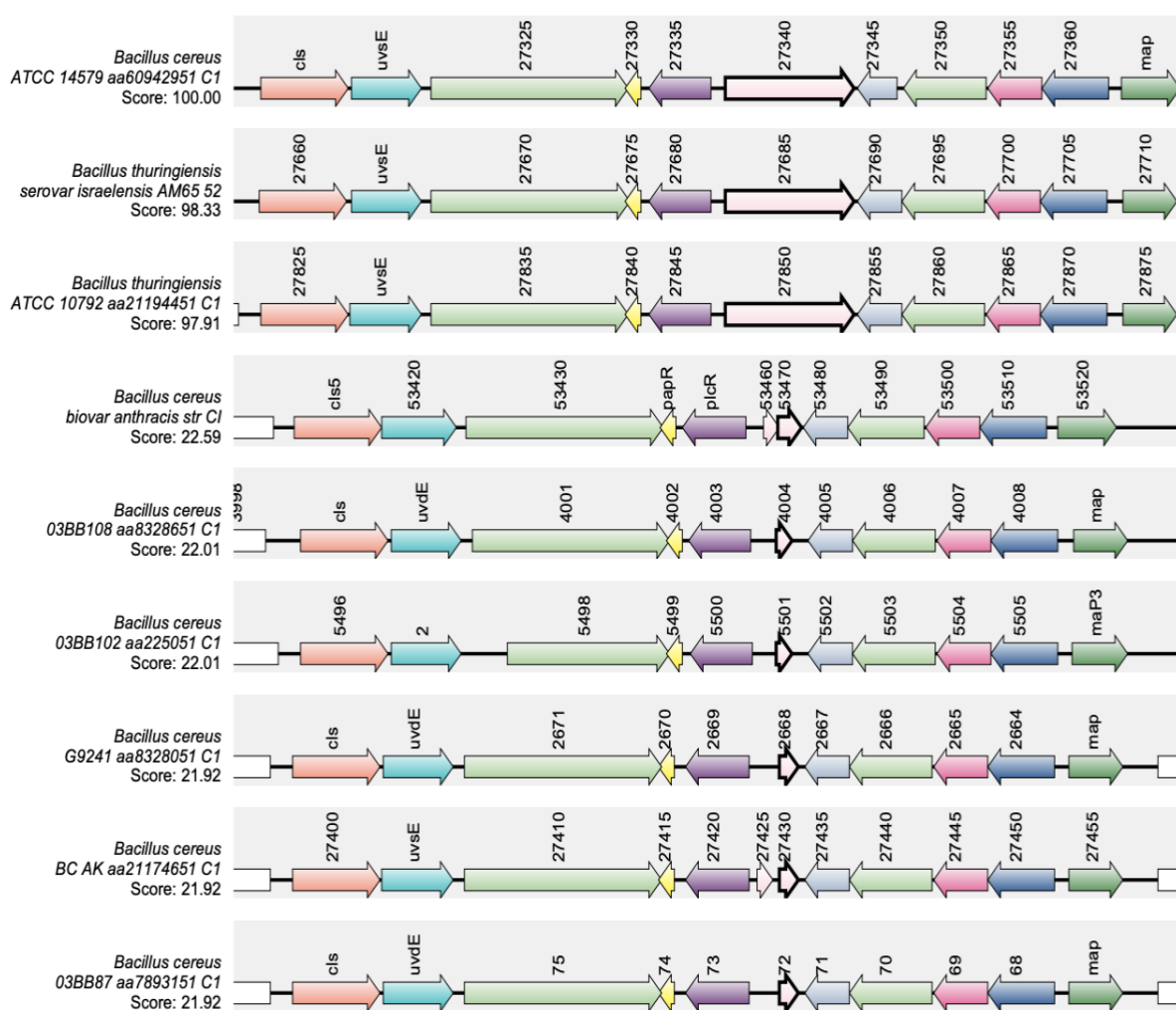
406 (<https://archaea.i2bc.paris-saclay.fr/SyntTax/Default.aspx>) was carried out. SyntTax uses the genomic  
407 and taxonomic database obtained from NCBI. The NprB protein sequence from *Bc*ATCC14579 (RefSeq  
408 accession GCF\_000007835.1) was used as the query protein. As shown in **Fig 5**, *Bc*G9241 as well as  
409 the “cross-over” strains *B. cereus* 03BB87, *B. cereus* 03BB102, *B. cereus* BC-AK and *B. cereus* bv  
410 *anthracis* CI can be seen to encode only remnants of the *nprB* gene located near the *plcR-papR* operon,  
411 with low synteny scores. In comparison, typical *B. cereus* sensu stricto and *B. thuringiensis* strains have  
412 intact copies of *nprB*, as previously described (6,21,22) with synteny scores above 97% (**Fig 5**). *B.*  
413 *anthracis* strains (Ames and Sterne) also lack the full copy of the *nprB* gene (22). This indicates that  
414 NprB may not be involved in processing PapR in *B. cereus* strains carrying functional copies of both  
415 *plcR* and *atxA*.

416  
417 This led us to question which protease(s) is/are capable of processing PapR in *Bc*G9241 and whether  
418 the temperature-dependent toxin expression in *Bc*G9241 is due to differential expression of these  
419 theoretical alternative protease enzymes. From the *Bc*G9241 secretome analysis of the supernatant  
420 extracted from cultures grown at 25 °C and 37 °C, several proteases were identified as highly expressed  
421 at 25 °C compared to 37 °C that could potentially be involved in processing PapR in *Bc*G9241 to its  
422 active form (**Table 1**). To determine whether temperature-dependent proteolytic activity is present in  
423 *Bc*G9241 as suggested by the secretome analysis, a protease activity assay was carried out using skim  
424 milk agar plates. Filtered supernatant of *Bc*G9241 grown at mid-exponential phase 25 °C showed  
425 hydrolysis of the skimmed milk casein whereas no clear zone was observed from cultures grown at  
426 mid-exponential phase 37 °C, which demonstrates that there is indeed a temperature-dependent  
427 protease activity deployed during mid-exponential phase of growth (**Fig 6**). Supernatants of *B. cereus*  
428 cultures into which synthetic PapR<sub>7</sub> was added were also collected and spotted onto skim milk agar to  
429 look for any changes in proteolytic activity. Interestingly, the addition of the synthetic PapR<sub>7</sub> peptide to  
430 cultures of either *Bc*G9241 or *Bc*G9241 Δ*pBCX01* led to a significant increase in proteolytic activity at  
431 both temperatures (**Fig S13**), presumably caused by PlcR-regulated proteases such as the thermolysin  
432 metallopeptidase (AQ16\_5317), which we have shown to be highly expressed at 25 °C compared to 37  
433 °C (see above).

434  
435 From the secretome analysis, AQ16\_5317 labelled as a thermolysin metallopeptidase was found to be  
436 highly abundant at 25 °C compared to 37 °C during exponential and stationary phase (**Table 1**). Out of  
437 all these proteases/enzymes listed in **Table 1**, only the gene encoding the thermolysin metallopeptidase  
438 and collagenase has a PlcR-box on the promoter region. There is a possibility that AQ16\_5317 is the  
439 protease involved in processing PapR in *Bc*G9241. From a synteny analysis to look into whether  
440 AQ16\_5317 thermolysin metallopeptidase was present in other *B. cereus* species, a high synteny score  
441 as shown in some of the *B. cereus*-*B. anthracis* “cross-over” strains, as well as *B. cereus* sensu stricto,  
442 *Bacillus weihenstephanensis*, *B. anthracis* and *B. thuringiensis* (**Fig S14**).

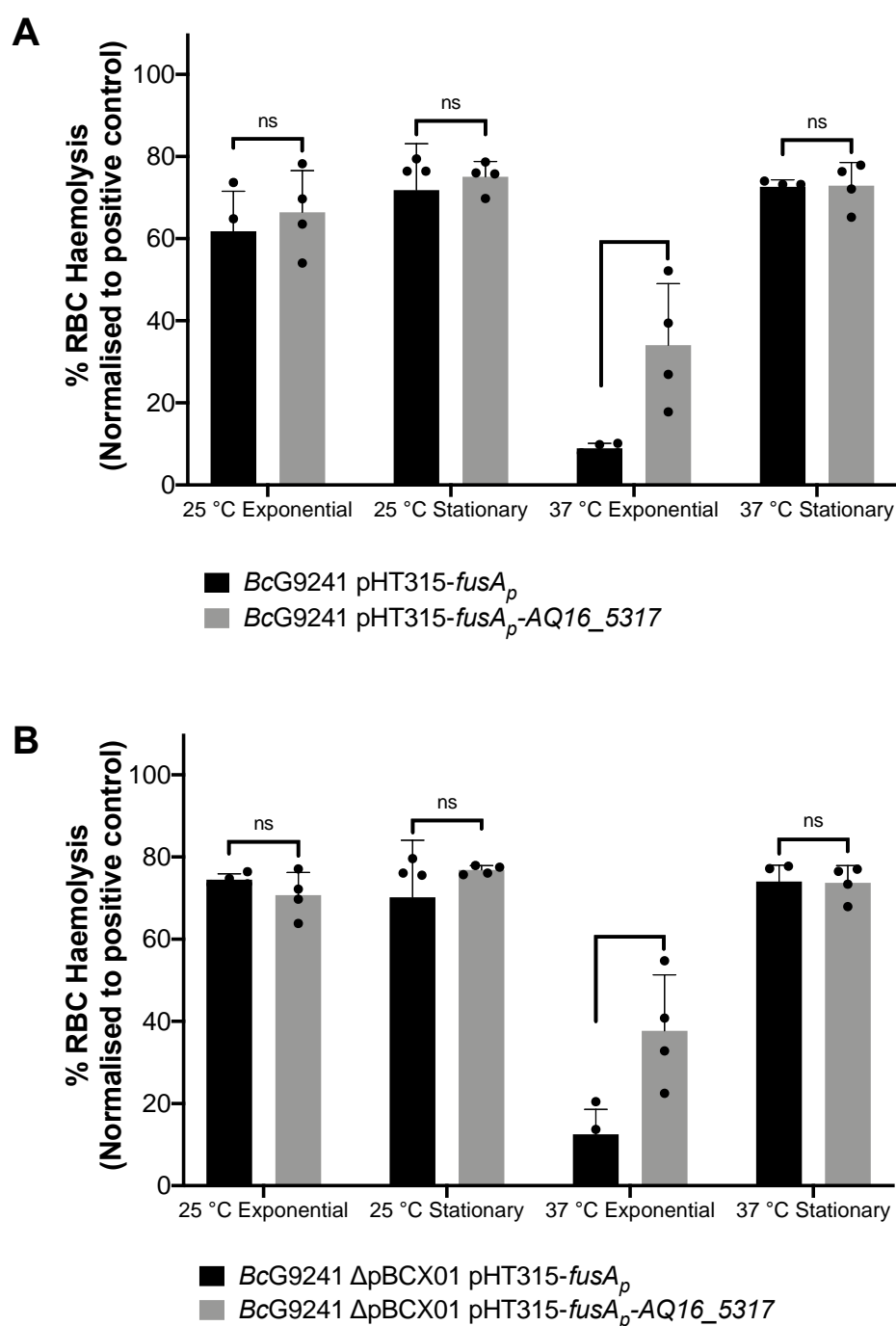
443  
444 To identify whether expressing AQ16\_5317 at 37 °C would abolish the temperature-dependent  
445 haemolytic phenotype, the AQ16\_5317 ORF with a promoter not linked to the PlcR-PapR regulator

446 (*fusA* promoter) was cloned into the shuttle vector pHT315 which should be able to constitutively  
 447 express the protease. When measuring the OD<sub>600</sub> over 24 hours using a plate reader, strains containing  
 448 the pHT315-*fusA<sub>P</sub>*-AQ16\_5317 construct did not alter the growth of the bacteria (data not shown). A  
 449 haemolysis assay using sheep erythrocytes was carried out with *BcG9241* strains containing the  
 450 constitutively expressed AQ16\_5317. Cell free culture supernatants from cultures grown at 25 °C and  
 451 37 °C from mid-exponential and stationary phase were tested in this assay. Supernatants from 25 °C  
 452 mid-exponential and early stationary phase cultures showed no change in haemolytic activity, with or  
 453 without the constitutive expression of AQ16\_5317. However, at 37 °C mid-exponential phase,  
 454 constitutive expression of AQ16\_5317 expressed at 37 °C led to a significant increase in haemolytic  
 455 activity compared to the control (**Fig 6**). The implication being that this protease is indeed capable of  
 456 processing PapR at 37 °C, leading to the increased expression of the PlcR regulon.



457  
 458 **Figure 5: Synteny of the gene encoding *nprB* in *B. cereus sensu stricto*, *B. thuringiensis*, *B.***  
 459 ***weihenstephanensis*, *B. cereus* “cross-over” strains and *B. anthracis*.** The NprB protein sequence  
 460 from *BcATCC14579* (RefSeq accession GCF\_000007835.1) was used as the query protein. The gene  
 461 encoding *nprB* is shown in pink with a bold border, *plcR* and *papR* are shown in purple and yellow,  
 462 respectively. SynTax, a synteny web service, was used to look in the conservation of gene order  
 463 (<https://archaea.i2bc.paris-saclay.fr/SyntTax/Default.aspx>).

464



465

466 **Figure 6: Slight increase in haemolytic activity with the presence of AQ16\_5317 at 37 °C during**  
 467 **exponential phase.** The haemolysis assay was conducted by incubating the supernatant of (A)  
 468 *BcG9241* and (B) *BcG9241* ΔpBCX01 with 4% RBC for one hour at 37 °C. OD<sub>540</sub> was measured and  
 469 RBC lysis was calculated as a percentage of expected RBC lysis, normalised with 70 % lysis from 1 %  
 470 (w/w) Triton X-100. Stars above columns represent significance levels: \* [P < 0.05] as determined by  
 471 unpaired t-test, with Welch's correction. Error bars denote one standard deviation, and all samples were  
 472 to an n=4.

473

## 474 DISCUSSION

475 The roles and expression of PlcR and AtxA are relatively well defined in *B. cereus* and *B. anthracis*,  
476 respectively. In *B. anthracis*, AtxA transcription and accumulation are enhanced at 37 °C compared to  
477 28 °C (49). In *B. cereus* and *B. thuringiensis*, PlcR transcription has been observed at the onset of  
478 stationary phase, suggesting cell density is required for transcription of the regulon (6,50). Also, the *B.*  
479 *weihenstephanensis* KBAB4 is reported to exhibit temperature-dependent production of PlcR and PlcR-  
480 regulated toxins (51). However, due to the rare nature of some *B. cereus* strains containing both *plcR*  
481 and *atxA* (9,10,38–42), the understanding of how a bacterium such as *BcG9241* has incorporated two  
482 hypothetically conflicting virulence regulators (8) has not yet been studied in detail.

483 Haemolysis and cytolysis assays using the supernatant of *BcG9241* demonstrated lytic activity at 25  
484 °C but not at 37 °C. The supernatant of *BcG9241* ΔpBCX01 also demonstrated temperature-dependent  
485 haemolytic and cytolytic activity, suggesting that this phenotype is not dependent on the pBCX01  
486 virulence plasmid encoding AtxA1. In comparison, the supernatant of *Bt Cry* Δ*plcR* and *Ba St* showed  
487 little or no cytotoxicity against a variety of eukaryotic cells at both temperatures. As *Bt Cry* Δ*plcR* and  
488 *Ba St* lack a functional *plcR* gene, it supports the hypothesis that PlcR-regulated toxins are responsible.  
489 Together these findings led us to propose that *BcG9241* ‘switches’ its phenotype from a haemolytic *B.*  
490 *cereus*-like phenotype at 25 °C to a non-haemolytic *B. anthracis*-like phenotype at 37 °C.

491  
492 The differential cytotoxicity pattern appears to be caused by the secretion of multiple cytolytic and  
493 haemolytic toxins at 25 °C, which includes Hbl, Nhe, Plc, CytK and a thermolysin metallopeptidase  
494 encoded by AQ16\_5317, detected from the secretome analysis of exponentially grown *BcG9241* cells.  
495 All the corresponding genes encode an upstream PlcR box sequence (**Table S1**) and are known to be  
496 transcriptionally regulated by PlcR in *BcATCC14579* (7,27). Using transcription-translation GFP  
497 reporters, we were able to confirm that *hbl::gfp*, *nhe::gfp*, *plc::gfp* and *AQ16\_5317::gfp* are expressed  
498 in a temperature dependent manner, with higher expression at 25 °C in *BcG9241*. This was also  
499 observed in *BcG9241* ΔpBCX01 (data not shown), further confirming that the temperature-dependent  
500 toxin production is independent of the virulence plasmid. In contrast, the expression of *hbl::gfp*, *nhe::gfp*  
501 and *BC\_2735::gfp* in *BcATCC14579* were at a similar level between the two temperatures. Expression  
502 of *cytK::gfp* in *BcG9241* was heterogeneous within the cell population, which Ceuppens *et al* (2012)  
503 also observed in *BcATCC14579* using a cyan fluorescent protein reporter (52).

504  
505 Interestingly, the most abundant proteins from the secretome analysis at 37 °C were phage proteins  
506 from the pBFH\_1 phagemid. This is in agreement with the transcriptomic data carried out by our group  
507 (13), where high transcript levels of genes encoded on the pBFH\_1 phagemid were identified at 37 °C  
508 compared to 25 °C from mid-exponentially grown *BcG9241* cells. It is possible that the expression of  
509 phage proteins might be interfering with normal PlcR-regulon toxin production. However, at this stage

510 we have not confirmed whether phage protein expression is the cause or the effect of a loss of PlcR-  
511 mediated toxin expression at 37 °C, or indeed entirely independent.

512

513 The cell proteome analysis of mid-exponentially grown *BcG9241* cells revealed no accumulation of  
514 toxins at 37 °C, implying that temperature-dependent toxin expression is not regulated at the level of  
515 secretion. Also, PlcR was detected at both temperatures from the cell proteome analysis with no  
516 significant difference between expression levels. Consequently, it can be concluded that the  
517 temperature-dependent toxin profile is not due to levels of PlcR in the cell. Instead, this suggests that  
518 the control point for temperature-dependent toxin secretion could be due to differential activity of the  
519 PlcR-PapR active complex.

520

521 In *BcG9241* and *BcATCC14579*, expression of PlcR using transcription-translation GFP reporters was  
522 first observed at the onset of stationary phase, in agreement with previous observations in *B.*  
523 *thuringiensis* (6). Expression of PlcR was highly heterogeneous during the onset of stationary phase  
524 and by 24 hours. As PlcR is under the direct- and indirect influence of other transcriptional regulators  
525 such as Spo0A and CodY (27,53), it is possible that these regulators play a role in the heterogeneous  
526 expression of PlcR. Phosphorylated Spo0A is able to inhibit the expression of PlcR due to the presence  
527 of two Spo0A-boxes between the PlcR box in the promoter region of *plcR* (27), while CodY controls the  
528 Opp system involved in importing processed PapR into the cell to activate PlcR (53). Population  
529 heterogeneity between genetically identical cells could be beneficial in order to survive, persist in  
530 fluctuating environment or be helpful for division of labour between cells. Transcription-translation  
531 expression of PapR using GFP reporters was also observed across the growth phase. Unexpectedly,  
532 expression of PapR in *BcG9241* increased dramatically at 37 °C, with a near homogenous expression  
533 observed by 24 hours. This is in contrast with what is observed in *BcATCC14579*, where the expression  
534 of PapR was heterogeneous at 25 °C and 37 °C. It is possible that at 37 °C, *BcG9241* cells are trying  
535 to compensate the low expression of the PlcR regulon by expressing PapR highly.

536

537 As analysis of the cell proteome did not show a build-up of toxins at 37 °C, we wanted to identify whether  
538 the temperature-dependent toxin production was caused by a limiting step within the PlcR-PapR  
539 regulatory circuit in *BcG9241*: import of mature PapR or processing of immature PapR.

540

541 Addition of synthetic PapR<sub>7</sub> to *BcG9241*, which would bypass the secretion and processing of the full-  
542 length peptide restored haemolytic activity at 37 °C. Supplementing the non-cognate form of the PapR<sub>7</sub>  
543 peptide into *B. cereus* strains led to suppression of haemolytic activity at both temperatures, confirming  
544 that the activating mechanism of PlcR-PapR is strain specific. This observation has been previously  
545 noted in *B. thuringiensis* (28). Using the PlcR-regulated toxin reporter strains made in this study, the  
546 addition of synthetic PapR<sub>7</sub> led to an increase in *nhe::gfp*, *plc::gfp* and *cytK::gfp* expression at 37 °C in  
547 *BcG9241*. This further confirms that the mature form of PapR can be imported into the cell at 37 °C in  
548 order to bind to PlcR and express the PlcR regulon. There was no significant increase in *hbl::gfp*  
549 expression at 37 °C with the addition of PapR<sub>7</sub>. This suggests that Nhe, Plc and CytK are responsible

550 for the haemolytic activity of *BcG9241* observed at 37 °C in the presence of PapR<sub>7</sub> (**Fig 4**). Intriguingly,  
551 the addition of PapR<sub>7</sub> at 25 °C led to a decrease in the expression of *hbl::gfp* in *BcG9241*. There is a  
552 possibility that there are other regulators that play a role in the expression of this enterotoxin such as  
553 ResDE (redox regulator), FnR, RpoN and Rex (54,55). It has been demonstrated that FnR, ResD and  
554 PlcR are able to form a ternary complex *in vivo* (56), which could explain the decrease of Hbl expression  
555 when synthetic PapR<sub>7</sub> were added.

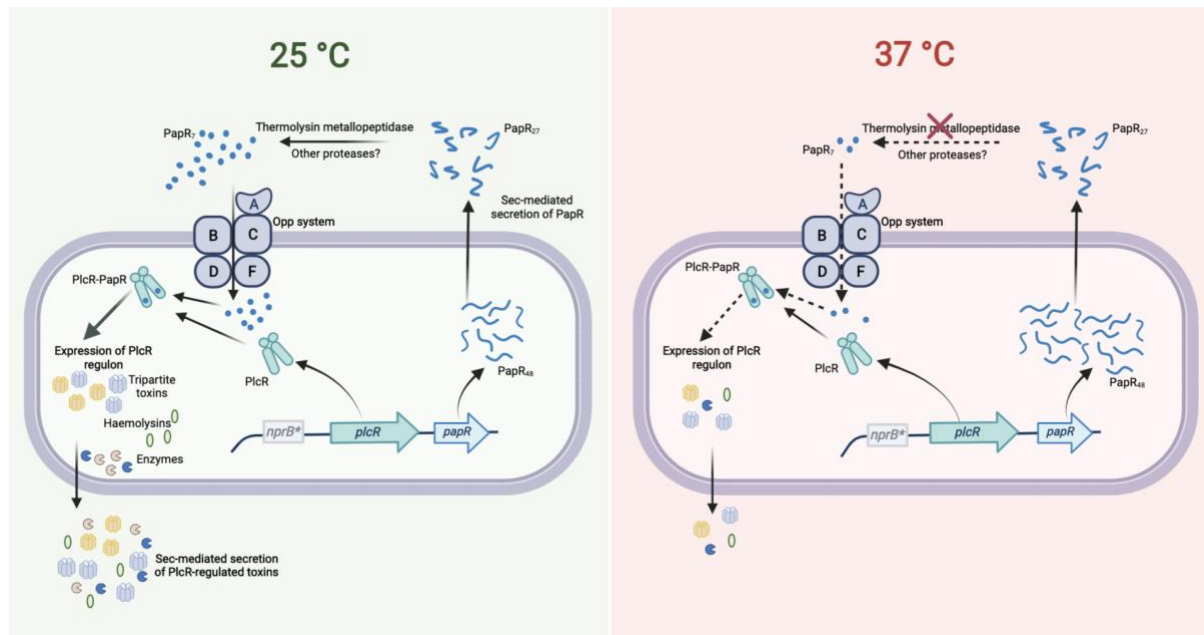
556

557 Finally, this led us to question as to whether the processing of PapR by an extracellular protease(s)  
558 was the limiting step causing the temperature-dependent toxin expression. The gene *nprB*, which  
559 encodes for the neutral protease involved in processing PapR in *B. cereus* and *B. thuringiensis* is  
560 truncated in *B. anthracis* (22), as well as in *BcG9241* and some of the *B. cereus*-*B. anthracis* “cross-  
561 over” strains that carry functional copies of *plcR-papR* and *atxA* (9,10,38–42). The loss of a functional  
562 copy of *nprB* may have contributed to the accommodation of *atxA* in these strains and potentially  
563 allowed *B. cereus*-*B. anthracis* “cross-over” strains to carry both regulators. Temperature-dependent  
564 proteolytic activity was observed using the supernatant of *BcG9241*, suggesting that the processing of  
565 PapR by extracellular proteases may be temperature-dependent manner. From the secretome analysis  
566 of *BcG9241*, AQ16\_5317, a thermolysin metallopeptidase, was found to be one of the most highly  
567 expressed proteases at 25 °C compared to 37 °C. Constitutive expression of AQ16\_5317 led to a slight  
568 increase in haemolytic activity at 37 °C, suggesting that AQ16\_5317 is capable of processing PapR into  
569 its mature form leading to the expression of PlcR-regulated toxins. The reason for not observing a  
570 similar level of haemolytic activity as observed using the supernatant extracted from 25 °C growth  
571 culture could be that AQ16\_5317 may require further processing in order to be in its active form or is  
572 not stable enough to carry out its function at 37 °C. It is also likely that though AQ16\_5317 is able to  
573 process PapR and express PlcR-regulated toxins at 37 °C, other proteases that have not been studied  
574 here can also carry out this function, and therefore further analysis is required. The possibility of other  
575 proteases processing immature PapR has been stated by Slamti *et al* (2014), though data have not  
576 been published to support this statement (57).

577

578 Overall, this study reveals that haemolytic and cytolytic activity in *BcG9241* is determined by  
579 temperature. Lytic activity at 25 °C was accompanied by higher levels of PlcR-regulated proteins  
580 including Hbl, Nhe, Plc, CytK and AQ16\_5317, a thermolysin metallopeptidase. Production of these  
581 virulence factors at 25 °C may be essential for the invasion of insect hosts. As shown in **Figure 7**,  
582 another finding of our work is that the temperature-dependent toxin production is due to differential  
583 expression of protease(s) involved in processing the immature PapR into its mature form to be  
584 reimported and then activate PlcR. This study suggests that temperature-dependent regulation of  
585 the PlcR-PapR regulator allows *BcG9241* to accommodate a functional copy of *atxA*. We hypothesise  
586 that this has led to the ability of *BcG9241* to switch between a *B. cereus*-like phenotype at 25 °C and a  
587 *B. anthracis*-like phenotype at 37 °C. The lower activity of the PlcR regulon at 37 °C compared to 25 °C  
588 could be to allow the expression of *AtxA* and its regulon, known to be expressed at 37 °C in *B. anthracis*  
589 (49). The characterisation of this “cross-over” strain demonstrates that the evolution of *B. anthracis* as

590 a significant mammalian pathogen is not merely about acquisition of genetic information but is also  
 591 story of the power of regulation in controlling potential incompatibilities between incumbent and newly  
 592 acquired systems which may be a feature of other emerging pathogens.



593  
 594 **Figure 7: The PlcR-PapR regulation circuit in *BcG9241* at 25 °C and 37 °C.** In *BcG9241*, the  
 595 expression of *plcR* was observed at 25 °C and 37 °C, suggesting that rather than the expression of the  
 596 regulator, the activity of the PlcR-PapR active complex is causing differential production of PlcR-  
 597 regulated toxins. PapR was highly expressed at 37 °C compared to 25 °C, potentially to compensate  
 598 for the low expression of the PlcR regulon. Secretion of PapR was observed at both temperatures,  
 599 suggesting that the Sec machinery is functional at both temperatures. The import system is also  
 600 functional at both temperatures when PapR<sub>7</sub> is available extracellularly. Remnants of the *nprB* gene  
 601 (*nprB*<sup>\*</sup>) are present in *BcG9241*, thus the protease NprB is not involved in the maturation of PapR as  
 602 observed in *B. cereus* and *B. thuringiensis*. A PlcR-regulated thermolysin metallopeptidase  
 603 (AQ16\_5317) was identified to have the ability to process PapR and cause haemolytic activity.  
 604 AQ16\_5317 is highly expressed at 25 °C compared to 37 °C. Diagram created with BioRender.com  
 605

## 606 MATERIALS AND METHODS

607

608 **Bacterial strains and growth conditions.** Bacterial strains used in this study were *BcG9241* (9),  
609 *BcG9241*  $\Delta$ pBCX01 (13), *B. cereus* reference strain ATCC 14579 (American Type Culture Collection,  
610 Manassas, Va.), the *plcR*-defective strain *B. thuringiensis* 407 Cry<sup>-</sup>  $\Delta$ *plcR* (18), and *B. anthracis* Sterne  
611 34F2 (pXO1<sup>+</sup>, pXO2<sup>-</sup>). *Bacillus* strains were cultured in 5 mL lysogeny broth (LB) at either 25 °C or 37  
612 °C overnight before subculturing into 5 mL LB media. All cultures were incubated with shaking at 200  
613 rpm. Larger cultures of *Bacillus* strains were cultured in 50 mL of LB unless otherwise specified. For  
614 cloning, *Escherichia coli* DH5- $\alpha$  (NEB) and the methylation deficient *E. coli* ET12567/pUZ8002 (58)  
615 were used in this study. *E. coli* strains were grown in 5 mL LB media at 37 °C, shaking at 200 rpm.  
616 Media contained antibiotics when appropriate: ampicillin (100  $\mu$ g/mL), chloramphenicol (25  $\mu$ g/mL),  
617 kanamycin (25  $\mu$ g/mL) for *E. coli* and erythromycin (25  $\mu$ g/mL) for *B. cereus* strains.

618

619 **Haemolysis assay.** Haemolytic activity was determined from sheep erythrocytes as described in  
620 (60). Briefly, erythrocytes were diluted to 4% (vol/vol), in RPMI-1640 medium and 50  $\mu$ L of this cell  
621 suspension were transferred to a 96-well round-bottom polystyrene plate and incubated with 50  $\mu$ L of  
622 filtered supernatants of *B. cereus* cells grown to exponential (OD<sub>600</sub>=0.5) or stationary phase  
623 (OD<sub>600</sub>=0.5). Following a 1 h-incubation at 37 °C, lysis of human/sheep erythrocytes were determined  
624 by quantifying the haemoglobin release by measurement of the absorbance at 540 nm in the resulting  
625 supernatant. LB and 1% Triton X-100 were used as negative and positive control for 0% lysis and 70%  
626 lysis, respectively. %RBC haemolysis was calculated as  $(OD_{\text{sample}} - OD_{\text{negative control}}) / (OD_{\text{positive control}} -$   
627  $OD_{\text{negative control}}) \times 70\%$ . Assays were done by triplicate unless otherwise stated.

628

629 **Protein extraction.** Before cultures were seeded for protein extraction, pre-cultures of *BcG9241* were  
630 used to synchronise bacterial cell growth. Pre-cultures were inoculated into 50 ml of LB broth at OD<sub>600</sub>  
631 = 0.005, for protein extraction. Secreted proteins were collected from mid-exponential phase or late  
632 stationary phase at both 25 °C and 37 °C. Once *BcG9241* had grown to the appropriate time point, 6.75  
633 OD units of cells were centrifuged for 5 minutes at 8000 rpm at 4 °C.

634

635 **(i) Protein extraction for secretome proteomics using in-gel digestion.** Supernatant was  
636 extracted and acidified to pH 5 using 10% trifluoroic acid (TFA). 50  $\mu$ L of StrataClean resin (Agilent) was  
637 added to each sample before vortexing for 1 minute. All samples were incubated overnight on a rotor  
638 wheel mixer overnight at 4 °C for efficient protein extraction. StrataClean resin was collected by  
639 centrifugation at 870 g for 1 minute. Cell supernatant was removed, and the beads resuspended in 100  
640  $\mu$ L of Laemlli buffer. The suspension was boiled at 95 °C for 5 minutes, to unbind the protein from the  
641 resin. Beads were pelleted at 870 g for 1 minute and protein-Laemlli buffer suspension collected.

642

643 25  $\mu$ L of the secreted proteins were ran on a Mini-PROTEAN® TGX™ precast gel (Bio-Rad). The whole  
644 lane of the gel for each sample was sliced into 4 mm sections and washed with 1 ml of 50% ethanol in



645 50 mM ammonium bicarbonate (ABC). This wash was incubated for 20 minutes at 55 °C, shaking at  
646 650 rpm. The wash solution was removed and this step was repeated twice more. The gel was  
647 dehydrated in 400 µl of 100% ethanol by incubation at 55 °C for 5 minutes, with 650 rpm shaking. Once  
648 the gel was dehydrated, remaining ethanol was removed. Disulphide bonds were reduced by addition  
649 of 300 µl of 10 mM dithiothreitol (DTT) in 50 mM ABC. This was incubated for 45 minutes at 56 °C with  
650 650 rpm shaking. DTT was removed and samples were cooled to room temperature. Cysteine residues  
651 were alkylated by adding 300 µl of 55 mM iodoacetamide (IAA) in 50 mM ABC with incubation at room  
652 temperature, in the dark for 30 minutes. IAA was removed and gel was washed as before by adding 1  
653 ml of 50% ethanol in 50 mM and incubated at 55 °C for 20 minutes with shaking at 650 rpm. The ethanol  
654 was removed and this wash was repeated twice. Gel pieces were again dehydrated with 400 µl of 100%  
655 ethanol and incubated for 5 minutes at 55 °C. 200 µl of trypsin at 2.5 ngµl<sup>-1</sup> was added to the dehydrated  
656 gel and ABC added to ensure the rehydrated gel was fully submerged. The trypsin digest was incubated  
657 for 16 hours at 37 °C with 650 rpm shaking. The digest was stopped by addition of 200 µl 5% formic  
658 acid in 25% acetonitrile. The solution was sonicated for 10 minutes at 35 KHz and the supernatant  
659 extracted. This step was repeated three more times. A C18 stage-tip (Thermo Scientific™) was made  
660 and conditioned by centrifuging 50 µl 100% methanol through the tip for 2 minutes at 2000 rpm. 100%  
661 acetonitrile was washed through the tip in the same manner to equilibrate it. The tip was further  
662 equilibrated with 2% acetonitrile with 1% TFA washed through the tip as before but for 4 minutes.  
663 Samples were then diluted to a concentration of 10 µg of protein in 150 µl final volume of 2%  
664 acetonitrile/0.1% TFA. Samples were collected on the stage tip by centrifugation through the stage tip  
665 for 10 minutes under previous spin conditions. The membrane was washed with 50 µl 2%  
666 acetonitrile/0.1% TFA by centrifugation at 2000 rpm for 4 minutes. Peptides were eluted in 20 µl 80%  
667 acetonitrile. Samples were dried to a total volume of 40 µl at 40 °C in a speed-vac. Samples were  
668 resuspended in 55 µl of 2.5% acetonitrile containing 0.05% TFA and sonicated for 30 minutes at 35  
669 KHz. Samples were dried to a total volume of 40 µl at 40 °C in a speed-vac again ready for mass  
670 spectroscopy. Nano liquid chromatography-electrospray ionisation-mass spectrometry (nanoLC-ESI-  
671 MS)/mass spectrometry (MS) was used to carry out the analysis.

672

673 **(ii) Protein extraction for intracellular proteomics using in-urea protein digests.** Cell  
674 supernatant was removed and cell pellets were suspended in 100 µl of 8M urea. Suspensions were  
675 transferred to Lysing Matrix B tubes (MP Biomedicals) and cells were lysed using the FastPrep®-24  
676 Classic instrument with a COOLPREP™ adapter (MP Biomedicals). Bead beating was conducted at 6  
677 ms<sup>-1</sup> for 40 s for 2 cycles, with a 300 s pause between cycles. Samples were filtered through  
678 nitrocellulose membranes to remove the beads and protein was quantified using a Qubit 2.0 fluorometer  
679 and a Qubit™ protein assay kit (Life Technologies). 50 µg of protein sample was suspended in 50 µl of  
680 8 M urea buffer. 5.5 µl of 10 mM DTT was added the samples were incubated for 1 hour at room  
681 temperature. 6.2 µl of 55 mM IAA was added to samples before 45 minutes incubation at room  
682 temperature in the dark. Samples were then diluted to 100 µL total volume by addition of 50 mM ABC.  
683 1 µg of trypsin was added to each sample per 50 µg protein and incubated for 16 hours at room  
684 temperature. Samples were filtered through a C-18 stage tip as described previously and concentrated

685 to 40  $\mu$ l in a speed-vac, ready for mass spectroscopy. nanoLC-ESI-MS/MS was used to carry out the  
686 analysis.

687

688 **Perseus analysis of proteomics data.** The Perseus software platform (Max Planck Institute) was  
689 used to analyse the highly multivariate proteomics data. Peptides only identified by site, reversed  
690 peptide sequences and potential contaminants were filtered out. Secretome data was normalised by  
691 the mean label-free quantification (LFQ) intensity value. Whole cell proteomics data was normalised by  
692 median as the data was normally distributed. Protein hits were filtered out if they didn't have 3 values  
693 in at least one condition measured. Volcano plots were plotted using a p value = 0.05 and a log2-fold  
694 change = 1.

695

696 **Generation of plasmid-based transcription-translation GFP reporters.** Constructs made for this  
697 study are listed on **Table S2**. Transcription-translation fusions with the *gfp* gene were constructed by  
698 PCR in a pHT315 vector (59) containing *gfp* (pHT315-*gfp*). The vector was linearized using appropriate  
699 restriction enzymes (NEB) and purified after agarose gel electrophoresis using the GFX™ PCR DNA  
700 and Gel Band Purification Kit (GE Healthcare). Insert fragments were amplified with Q5 DNA  
701 polymerase (NEB) by PCR with the appropriate primer pairs listed on **Table S3**. The resulting fragments  
702 were digested with the appropriate restriction enzymes, purified after agarose gel electrophoresis using  
703 the GFX™ PCR DNA and Gel Band Purification Kit (GE Healthcare) and ligated into  
704 the linearized pHT315-*gfp* vector. Plasmid constructs were transformed into chemically competent *E.*  
705 *coli* DH5- $\alpha$  cells through heat shock. Once confirmed by DNA sequencing, all vectors were transformed  
706 into the non-methylating *E. coli* ET12567 strain by electroporation (**Supplementary Materials and**  
707 **Methods**). Vectors amplified by *E. coli* ET12567 were purified and transformed into *B. cereus* strains  
708 using electroporation (**Supplementary Materials and Methods**).

709

710 **Fluorescent reporter strain assays.** For growth curves and fluorescence measurements, *B. cereus*  
711 strains were sub-cultured at a starting OD<sub>600</sub> of 0.05 into a clear flat bottom 96-well plate (Greiner)  
712 containing 100  $\mu$ L of LB media per well. Cultures were grown in a FLUOstar Omega microplate reader  
713 (BMG LabTech) at either 25 °C or 37 °C with continuous orbital shaking at 700 rpm. Absorbance  
714 measurements (OD<sub>600</sub>) and fluorescence intensity (excitation filter = 482 nm and emission filter = 520  
715 nm for GFP) were taken hourly for 24 hours. Each plate contained *BcG9241* and *BcATCC14579* strains  
716 carrying GFP reporters as well as each strain carrying a control plasmid with no promoter upstream of  
717 *gfp* (pHT315-*gfp*). The fluorescence of all readings was first normalized to the fluorescence of blank  
718 media samples and then normalized by subtracting the autofluorescence of the corresponding control  
719 strain. The rate of change in fluorescence ( $\Delta$ GFP/OD<sub>600</sub>) using the data obtained from the microplate  
720 reader was calculated by subtracting the fluorescence at a given time point by the fluorescence of the  
721 previous time point:

722

$$\Delta\text{GFP}/\text{OD}_{600} = (\text{GFP intensity}_{(t)} - \text{GFP intensity}_{(t-1)})/\text{OD}_{600}$$

723

724 **Peptide Synthesis.** Peptides SDLPFEH (G9241 PapR<sub>7</sub>) and KDLPFEY (ATCC14579 PapR<sub>7</sub>) were  
725 synthesised by GenScript (USA) at a purity >98% and diluted with sterile nuclease-free water. All  
726 experiments with the use of PapR<sub>7</sub> were added at a concentration of 10 µM and during lag growth phase  
727 (OD<sub>600</sub> = 0.1), unless otherwise stated.

728

729 **Light and Fluorescence Microscopy.** 1 % agarose in water were made and heated using a  
730 microwave until the agarose has completely dissolved. 200 µl of molten agarose was added onto a  
731 microscope glass slide and a coverslip placed on top. When the agarose pad has dried and the sample  
732 is ready for observation, 2 µl of sample was applied to a prepared agarose pad and a cover slip placed  
733 over them. Images were captured on a Leica DMI8 premium-class modular research microscope with  
734 a Leica EL6000 external light source (Leica Microsystems), using an ORCA-Flash4.0 V2 Digital CMOS  
735 Camera (Hamamatsu) at 100x magnification.

736

737 **PapR<sub>7</sub> activity assay using PlcR-regulated toxin reporters.** *BcG9241* and *BcATCC14579*  
738 containing PlcR-regulated toxin GFP reporters were grown overnight in LB medium with selective  
739 antibiotics. Mid-exponentially grown pre-cultures of *B. cereus* strains containing PlcR-regulated toxin  
740 reporters were diluted to OD<sub>600</sub> 0.01 and 10 µM of PapR<sub>7</sub> were added. In a black tissue culture treated  
741 96-well microtiter plate (Greiner, Scientific Laboratory Supplies), 100 µL of the culture were added in  
742 each well and the GFP intensity and OD<sub>600</sub> were measured every hour for over 24 hours using the  
743 Omega FluoSTAR (BMG LabTech) microplate reader.

744

## 745 **AUTHORS AND CONTRIBUTORS**

746 **Shathviga Manoharan**<sup>1</sup>: Planned and performed experiments and wrote much of the manuscript

747 **Grace Taylor-Joyce**<sup>1</sup>: Assisted in experiments and wrote parts of the manuscript

748 **Thomas Brooker**<sup>1</sup>: Planned and performed some of the experiments.

749 **Carmen Sara Hernandez-Rodriguez**<sup>2</sup>: Planned and performed some of the experiments.

750 **Les Baillie**<sup>3</sup>: Provided certain bacterial strains and provided advice on handling them.

751 **Petra Oyston and Victoria Baldwin**<sup>4</sup>: Provided advice on handling the pathogenic strains and  
752 assisted in interpreting the results.

753 **Alexia Hapeshi**<sup>1</sup>: Assisted in some experimental work and in interpreting certain results.

754 **Nicholas R. Waterfield**<sup>1</sup>: Experimental planning, secured funding, assisted in interpreting results and  
755 provided guidance and edits for writing the manuscript.

756

757 <sup>1</sup>Division of Biomedical Sciences, Warwick Medical School, University of Warwick, Gibbet Hill Road,  
758 Coventry, CV4 7AL, United Kingdom

759 <sup>2</sup>Institut Universitari de Biotecnologia i Biomedicina, Departament de Genètica, Facultat de Ciències  
760 Biològiques, University of Valencia, 46100 Burjassot, Valencia, Spain

761 <sup>3</sup>School of Pharmacy and Pharmaceutical Sciences, Cardiff University, CF10 3AT, Cardiff, United  
762 Kingdom

763 <sup>4</sup>CBR Division, Dstl Porton Down, Salisbury, SP4 0JQ, United Kingdom

764

765

## 766 **CONFLICTS OF INTEREST**

767 The authors declare no conflicts of interest.

768

## 769 **FUNDING INFORMATION**

770 **SM** and **TB** were funded by the WCPRS scholarship programme provided by Warwick University, with  
771 funding contributions from Dstl (MoD) at Porton Down, UK (DSTL project references;  
772 DSTLX1000093952 and DSTLX-1000128995). **GTJ** was funded by the BBSRC MIBTP Doctoral  
773 Training Programme at the University of Warwick, UK. **CSHR** was funded by an EU Marie Curie  
774 fellowship awarded while at the University of Bath, UK (FP7-PEOPLE-2010-IEF Project 273155). **AH**  
775 was funded by a start-up financial package awarded to **NRW** upon starting at Warwick Medical School,  
776 UK. **LB** is funded by Cardiff School of Biological Sciences, UK. **PO** is funded by Dstl at Porton Down,  
777 UK. **NRW** is funded by the University of Warwick, UK.

778

## 779 **ACKNOWLEDGEMENTS**

780 We would like to thank the Dstl for providing funding and guidance throughout the project including  
781 valuable quarterly update meetings. We would also like to acknowledge the contribution of the WPH  
782 Proteomics Research Technology Platform (Gibbet Hill Road, University of Warwick, UK).

783

## 784 **REFERENCES**

- 785 1. Vilain S, Luo Y, Hildreth MB, Brözel VS. Analysis of the life cycle of the soil Saprophyte *Bacillus cereus* in  
786 liquid soil extract and in soil. *Appl Environ Microbiol*. 2006;72(7):4970–7.
- 787 2. Okinaka R, Keim P. The Phylogeny of *Bacillus cereus* sensu lato. *Microbiol Spectr*. 2016;4(1).
- 788 3. Carter KC. Koch's Postulates in Relation To the Work of Jacob Henle and Edwin Klebs. *Med Hist*.  
789 1985;29:353–74.
- 790 4. Swiecicka I, Mahillon J. Diversity of commensal *Bacillus cereus* sensu lato isolated from the common sow  
791 bug (*Porcellio scaber*, *Isopoda*). *FEMS Microbiol Ecol*. 2006;56(1):132–40.
- 792 5. Granum PE, Lund T. *Bacillus cereus* and its food poisoning toxins. *FEMS Microbiol Lett*. 1997;157(2):223–  
793 8.
- 794 6. Lereclus D, Agaisse H, Gominet M, Salamitou S, Sanchis V. Identification of a *Bacillus thuringiensis* Gene  
795 That Positively Regulates Transcription of the Phosphatidylinositol-Specific Phospholipase C Gene at the  
796 Onset of the Stationary Phase. *J Bacteriol*. 1996;178(10):2749–56.
- 797 7. Agaisse H, Gominet M, Økstad OA, Kolstø AB, Lereclus D. PlcR is a pleiotropic regulator of extracellular  
798 virulence factor gene expression in *Bacillus thuringiensis*. *Mol Microbiol*. 1999;32(5):1043–53.
- 799 8. Mignot T, Mock M, Robichon D, Landier A, Lereclus D, Fouet A. The incompatibility between the PlcR- and  
800 AtxA-controlled regulons may have selected a nonsense mutation in *Bacillus anthracis*. *Mol Microbiol*.  
801 2001;42(5):1189–98.
- 802 9. Hoffmaster AR, Ravel J, Rasko DA, Chapman GD, Chute MD, Marston CK, et al. Identification of anthrax

- 803 toxin genes in a *Bacillus cereus* associated with an illness resembling inhalation anthrax. Proc Natl Acad  
804 Sci U S A. 2004 Jun 1;101(22):8449–54.
- 805 10. Hoffmaster AR, Hill KK, Gee JE, Marston CK, De BK, Popovic T, *et al.* Characterization of *Bacillus cereus*  
806 isolates associated with fatal pneumonias: Strains are closely related to *Bacillus anthracis* and Harbor *B.*  
807 *anthracis* virulence genes. J Clin Microbiol. 2006;44(9):3352–60.
- 808 11. Visschedyk D, Rochon A, Tempel W, Dimov S, Park HW, Merrill AR. Certhrax toxin, an anthrax-related  
809 ADP-ribosyltransferase from *Bacillus cereus*. J Biol Chem. 2012;287(49):41089–102.
- 810 12. Fieldhouse RJ, Turgeon Z, White D, Rod Merrill A. Cholera- and anthrax-like toxins are among several  
811 new ADP-Ribosyltransferases. PLoS Comput Biol. 2010;6(12).
- 812 13. Taylor-Joyce G, Manoharan S, Brooker T, Hernandez-Rodriguez CS, Baillie L, Oyston P, Waterfield, N. R.  
813 The influence of extrachromosomal elements in the anthrax “cross-over” strain *Bacillus cereus* G9241.  
814 [Unpublished manuscript]. University of Warwick. 2022.
- 815 14. Hendrix RW, Casjens SR, Lavigne R. Family - Siphoviridae. Virus Taxon Ninth Rep Int Comm Taxon  
816 Viruses. 2012.
- 817 15. Gohar M, Økstad OA, Gilois N, Sanchis V, Kolstø AB, Lereclus D. Two-dimensional electrophoresis  
818 analysis of the extracellular proteome of *Bacillus cereus* reveals the importance of the PlcR regulon.  
819 Proteomics. 2002;2(6):784–91.
- 820 16. Gohar M, Faegri K, Perchat S, Ravnum S, Økstad OA, Gominet M, *et al.* The PlcR virulence regulon of  
821 *Bacillus cereus*. PLoS One. 2008;3(7):1–9.
- 822 17. Clair G, Roussi S, Armengaud J, Duport C. Expanding the Known Repertoire of Virulence Factors  
823 Produced by *Bacillus cereus* through Early Secretome Profiling in Three. Mol Cell Proteomics.  
824 2010;9(7):1486–98.
- 825 18. Salamitou S, Brehe M, Bourguet D, Gilois N, Gominet M, Hernandez E. The PlcR regulon is involved in  
826 the opportunistic properties of *Bacillus thuringiensis* and *Bacillus cereus* in mice and insects. Microbiology.  
827 2000;146:2825–32.
- 828 19. Bouillaut L, Perchat S, Arold S, Zorrilla S, Slamti L, Henry C, *et al.* Molecular basis for group-specific  
829 activation of the virulence regulator PlcR by PapR heptapeptides. Nucleic Acids Res. 2008;36(11):3791–  
830 801.
- 831 20. Slamti L, Gominet M, Vilas-bo G, Sanchis V, Chaufaux J, Gohar M, *et al.* Distinct Mutations in PlcR Explain  
832 Why Some Strains of the *Bacillus cereus* Group are Nonhemolytic. J Bacteriol. 2004;186(11):3531–8.
- 833 21. Økstad OA, Gominet M, Purnelle B, Rose M, Lereclus D, Kolsto A-B. Sequence analysis of three *Bacillus*  
834 *cereus* loci carrying PlcR-regulated genes encoding degradative enzymes and enterotoxin. Microbiology.  
835 1999;145:3129–38.
- 836 22. Pomerantsev AP, Pomerantseva OM, Camp AS, Mukkamala R, Goldman S, Leppla SH. PapR peptide  
837 maturation : Role of the NprB protease in *Bacillus cereus* 569 PlcR / PapR global gene regulation. FEMS  
838 Immunol Med Microbiol. 2009;55:361–77.
- 839 23. Gominet M, Slamti L, Gilois N, Rose M, Lereclus D, Universita È. Oligopeptide permease is required for  
840 expression of the *Bacillus thuringiensis* PlcR regulon and for virulence. Mol Microbiol. 2001;40(4):963–75.
- 841 24. Slamti L, Lereclus D. A cell-cell signaling peptide activates the PlcR virulence regulon in bacteria of the  
842 *Bacillus cereus* group. EMBO J. 2002;21(17):4550–9.
- 843 25. Declerck N, Bouillaut L, Chaix D, Rugani N, Slamti L, Hoh F, *et al.* Structure of PlcR: Insights into virulence  
844 regulation and evolution of quorum sensing in Gram-positive bacteria. PNAS. 2007;104(47):18490–5.
- 845 26. Grenha R, Slamti L, Nicaise M, Refes Y, Lereclus D, Nessler S. Structural basis for the activation  
846 mechanism of the PlcR virulence regulator by the quorum-sensing signal peptide PapR. PNAS.  
847 2013;110(3):1047–52.

- 848 27. Lereclus D, Agaisse H, Salamitou S, Gominet M. Regulation of toxin and virulence gene transcription in  
849 *Bacillus thuringiensis*. Int J Med Microbiol. 2000;290(4–5):295–9.
- 850 28. Slamti L, Lereclus D. Specificity and Polymorphism of the PlcR-PapR Quorum-Sensing System in the  
851 *Bacillus cereus* Group. J Bacteriol. 2005;187(3):1182–7.
- 852 29. Gilmore MS, Cruz-Rodz AL, Leimeister-Wachter M, Kreft J, Goebel W. A *Bacillus cereus* cytolytic  
853 determinant, cereolysin AB, which comprises the phospholipase C and sphingomyelinase genes:  
854 Nucleotide sequence and genetic linkage. J Bacteriol. 1989;171(2):744–53.
- 855 30. Lund T, Granum PE. Characterisation of a non-haemolytic enterotoxin complex from *Bacillus cereus*  
856 isolated after a foodborne outbreak. FEMS Microbiol Lett. 1996;141:151–6.
- 857 31. Lund T, De Buyser M-L, Granum PE. A new cytotoxin from *Bacillus cereus* that may cause necrotic  
858 enteritis. Mol Microbiol. 2000;38(2):254–61.
- 859 32. Leendertz FH, Yumlu S, Pauli G, Boesch C, Couacy-Hymann E, Vigilant L, et al. A new *Bacillus anthracis*  
860 found in wild chimpanzees and a gorilla from west and central Africa. PLoS Pathog. 2006;2(1):0001–4.
- 861 33. Antonation KS, Grützmacher K, Dupke S, Mabon P, Zimmermann F, Lankester F, et al. *Bacillus cereus*  
862 Biovar Anthracis Causing Anthrax in Sub-Saharan Africa—Chromosomal Monophyly and Broad  
863 Geographic Distribution. PLoS Negl Trop Dis. 2016;10(9):1–14.
- 864 34. Leendertz FH, Ellerbrok H, Boesch C, Couacy-Hymann E, Mätz-Rensing K, Haken, et al. Anthrax kills wild  
865 chimpanzees in a tropical rainforest. Nature. 2004;430:451–2.
- 866 35. Leendertz FH, Lankester F, Guislain P, Neel C, Drori O. Anthrax in Western and Central African Great  
867 Apes. Am J Primatol. 2006;68:928–33.
- 868 36. Klee SR, Brzuszkiewicz EB, Nattermann H, Brüggemann H, Dupke S, Wollherr A, et al. The genome of a  
869 *Bacillus* isolate causing anthrax in chimpanzees combines chromosomal properties of *B. cereus* with *B.*  
870 *anthracis* virulence plasmids. PLoS One. 2010;5(7):e10986.
- 871 37. Miller JM, Hair JG, Hebert M, Hebert L, Roberts Jr. FJ, Weyant RS. Fulminating bacteremia and pneumonia  
872 due to *Bacillus cereus*. J Clin Microbiol. 1997;35(2):504–7.
- 873 38. Sue D, Hoffmaster AR, Popovic T, Wilkins PP. Capsule production in *Bacillus cereus* strains associated  
874 with severe pneumonia. J Clin Microbiol. 2006;44(9):3426–8.
- 875 39. Avashia SB, Riggins WS, Lindley C, Hoffmaster A, Drumgoole R, Nekomoto T, et al. Fatal Pneumonia  
876 among Metalworkers Due to Inhalation Exposure to *Bacillus cereus* Containing *Bacillus anthracis* Toxin  
877 Genes. Clin Infect Dis. 2007;44:414–6.
- 878 40. Marston CK, Ibrahim H, Lee P, Churchwell G, Gumke M, Stanek D, et al. Anthrax toxin-expressing *Bacillus*  
879 *cereus* isolated from an anthrax-like eschar. PLoS One. 2016;11(6):1–7.
- 880 41. Wright AM, Beres SB, Consamus EN, Long SW, Flores AR, Barrios R, et al. Rapidly Progressive, Fatal,  
881 Inhalation Anthrax-like Infection in a Human: Case Report, Pathogen Genome Sequencing, Pathology,  
882 and Coordinated Response. Arch Pathol Lab Med. 2011;1447–59.
- 883 42. Pena-Gonzalez A, Marston CK, Rodriguez-R LM, Kolton CB, Garcia-Diaz J, Theppote A, et al. Draft  
884 genome sequence of *Bacillus cereus* LA2007, a human-pathogenic isolate harboring anthrax-like  
885 plasmids. Genome Announc. 2017;5(16).
- 886 43. Dupke S, Barduhn A, Franz T, Leendertz FH, Couacy-Hymann E, Grunow R, et al. Analysis of a newly  
887 discovered antigen of *Bacillus cereus* biovar *anthracis* for its suitability in specific serological antibody  
888 testing. J Appl Microbiol. 2019;126(1):311–23.
- 889 44. Dawson P, Schrodtt CA, Feldmann K, Traxler RM, Gee JE, Kolton CB, et al. Fatal Anthrax Pneumonia in  
890 Welders and Other Metalworkers Caused by *Bacillus cereus* Group Bacteria Containing Anthrax Toxin  
891 Genes — U.S. Gulf Coast States, 1994–2020. Morb Mortal Wkly Rep. 2021;70(41):1453–4.
- 892 45. Baldwin VM. You Can't *B. cereus* – A Review of *Bacillus cereus* Strains That Cause Anthrax-Like Disease.

- 893 Front Microbiol. 2020;11(1731).
- 894 46. Passalacqua KD, Varadarajan A, Byrd B, Bergman NH. Comparative transcriptional profiling of *Bacillus*  
895 *cereus* sensu lato strains during growth in CO<sub>2</sub>-bicarbonate and aerobic atmospheres. PLoS One.  
896 2009;4(3):1–20.
- 897 47. Rivera AMG, Granum PE, Priest FG. Common occurrence of enterotoxin genes and enterotoxicity in  
898 *Bacillus thuringiensis*. FEMS Microbiol Lett. 2000;190(1):151–5.
- 899 48. Swiecicka I, Van Der Auwera GA, Mahillon J. Hemolytic and nonhemolytic enterotoxin genes are broadly  
900 distributed among *Bacillus thuringiensis* isolated from wild mammals. Microb Ecol. 2006;52(3):544–51.
- 901 49. Dai Z, Koehler TM. Regulation of Anthrax Toxin Activator Gene (*atxA*) Expression in *Bacillus anthracis*:  
902 Temperature, Not CO<sub>2</sub>/ Bicarbonate, Affects *AtxA* Synthesis. Infect Immun. 1997;65(7):2576–82.
- 903 50. Brillard J, Susanna K, Michaud C, Dargaignaratz C, Gohar M, Nielsen-Leroux C, et al. The YvFTU two-  
904 component system is involved in *plcR* expression in *Bacillus cereus*. BMC Microbiol. 2008;8:1–13.
- 905 51. Réjasse A, Gilois N, Barbosa I, Huillet E, Bevilacqua C, Tran S, et al. Temperature-Dependent Production  
906 of Various *PlcR*-Controlled Virulence Factors in *Bacillus weihenstephanensis* Strain KBAB4. Appl Environ  
907 Microbiol. 2012;78(8):2553–61.
- 908 52. Ceuppens S, Timmerly S, Mahillon J, Uyttendaele M, Boon N. Small *Bacillus cereus* ATCC 14579  
909 subpopulations are responsible for cytotoxin K production. J Appl Microbiol. 2012;114(3):899–906.
- 910 53. Slamti L, Lemy C, Henry C, Guillot A, Huillet E, Lereclus D. CodY regulates the activity of the virulence  
911 quorum sensor *PlcR* by controlling the import of the signaling peptide *PapR* in *Bacillus thuringiensis*. Front  
912 Microbiol. 2016;6(1501):1–14.
- 913 54. Duport C, Zigha A, Rosenfeld E, Schmitt P. Control of enterotoxin gene expression in *Bacillus cereus*  
914 F4430/73 involves the redox-sensitive ResDE signal transduction system. J Bacteriol. 2006;188(18):6640–  
915 51.
- 916 55. Zigha A, Rosenfeld E, Schmitt P, Duport C. The redox regulator *Fnr* is required for fermentative growth  
917 and enterotoxin synthesis in *Bacillus cereus* F4430/73. J Bacteriol. 2007;189(7):2813–24.
- 918 56. Esbelin J, Jouanneau Y, Duport C. *Bacillus cereus* *Fnr* binds a [4Fe-4S] cluster and forms a ternary  
919 complex with ResD and *PlcR*. BMC Microbiol. 2012;12(125).
- 920 57. Slamti L, Perchat S, Huillet E, Lereclus D. Quorum sensing in *Bacillus thuringiensis* is required for  
921 completion of a full infectious cycle in the insect. Toxins (Basel). 2014;6(8):2239–55.
- 922 58. MacNeil DJ, Gewain KM, Ruby CL, Dezeny G, Gibbons PH, MacNeil T. Analysis of *Streptomyces*  
923 *avermitilis* genes required for avermectin biosynthesis utilizing a novel integration vector. Gene.  
924 1992;111(1):61–8.
- 925 59. Wilson MK, Vergis JM, Alem F, Palmer JR, Keane-Myers AM, Brahmabhatt TN, et al. *Bacillus cereus* G9241  
926 makes anthrax toxin and capsule like highly virulent *B. anthracis* Ames but behaves like attenuated  
927 toxigenic nonencapsulated *B. anthracis* Sterne in rabbits and mice. Infect Immun. 2011;79(8):3012–9.
- 928 60. Rudkin JK, Laabei M, Edwards AM, Joo HS, Otto M, Lennon KL, et al. Oxacillin alters the toxin expression  
929 profile of community-associated methicillin-resistant *Staphylococcus aureus*. Antimicrob Agents  
930 Chemother. 2014;58(2):1100–7.
- 931 61. Lane DL. 16S/23S rRNA sequencing. Nucleic Acid Techniques in Bacterial Systematics. 1991;115–75.
- 932 62. Arantes O, Lereclus D. Construction of cloning vectors for *Bacillus thuringiensis*. Gene. 1991;108:115–9.
- 933 63. Salter RD, Cresswell P. Impaired assembly and transport of HLA-A and -B antigens in a mutant TxB cell  
934 hybrid. EMBO J. 1986;5(5):943–9.
- 935 64. Daigneault M, Preston JA, Marriott HM, Whyte MKB, Dockrell DH. The identification of markers of  
936 macrophage differentiation in PMA-stimulated THP-1 cells and monocyte-derived macrophages. PLoS  
937 One. 2010;5(1).

- 938 65. Silva, C.P., Waterfield, N.R., Daborn, P.J., Dean, P., Chilver, T., Au, C.P.Y., Sharma, S., Potter, U.,  
939 Reynolds, S.E. and Ffrench-Constant, R.H. (2002) 'Bacterial infection of a model insect: *Photobacterium*  
940 *luminescens* and *Manduca sexta*', *Cellular Microbiology*, 4(6), pp. 329–339.
- 941 66. Vlisidou I, Hapeshi A, Healey JRJ, Smart K, Yang G, Waterfield NR. The *Photobacterium asymbiotica*  
942 virulence cassettes deliver protein effectors directly into target eukaryotic cells. *Elife*. 2019;8:1–24.  
943